PROCEEDINGS OF THE 24TH INTERNATIONAL APPLIED GEOCHEMISTRY SYMPOSIUM

FREDERICTON, NEW BRUNSWICK, CANADA

JUNE 1ST-4TH, 2009

EDITED BY

DAVID R. LENTZ, KATHLEEN G. THORNE, & KRISTY-LEE BEAL

VOLUME II

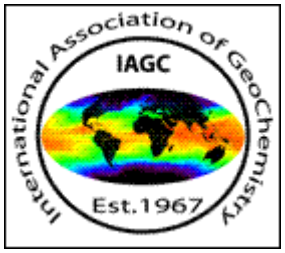

ISBN 978-1-55131-137-1 (Volume 2)

PROCEEDINGS OF THE 24TH INTERNATIONAL APPLIED GEOCHEMISTRY SYMPOSIUM

FREDERICTON, NEW BRUNSWICK
CANADA
JUNE 1ST-4TH, 2009

EDITED BY

DAVID R. LENTZ
KATHLEEN G. THORNE
KRISTY-LEE BEAL

VOLUME II

TECHNICAL EDITORS

(Listed in alphabetical order)

Mark Arundell
U. Aswathanarayana
Roger Beckie
Chris Benn
Robert Bowell
Charles Butt
Bill Coker
Hugh deSouza
Sara Fortner
David Gladwell
Wayne Goodfellow
Eric Grunsky
William Gunter
Gwendy Hall
Jacob Hanley
Russell Harmon
David Heberlein
Brian Hitchon
Andrew Kerr
Dan Kontak
Kurt Kyser
David Lentz
Ray Lett
Matthew Leybourne
Steven McCutcheon
Beth McClenaghan
Nancy McMillan
Paul Morris
Lee Ann Munk
Dogan Paktunc
Roger Paulen
Ernie Perkins
David Quirt
Andy Rencz
David Smith
Cliff Stanley
Gerry Stanley
Nick Susak
Bruce Taylor
Ed Van Hees
James Walker
Lawrence Winter

CURRENT CAPABILITIES AND FUTURE PROSPECTS OF REAL-TIME, IN-FIELD GEOCHEMICAL ANALYSIS

EDITED BY:

RUSSELL S. HARMON
NANCY MCMILLAN

LIBS-based geochemical fingerprinting for the rapid analysis and discrimination of minerals – the example of garnet

Daniel C. Alvey[1], Jeremiah J. Remus[2], Russell S. Harmon[3], Jennifer L. Gottfried[4], & Kenneth Morton[2]

[1] *U.S. Military Academy, West Point, NY, 10996 USA*
[2] *Electrical and Computer Engineering, Duke University, Durham, NC, 27708 USA*
[3] *ARL Army Research Office, 4300 S. Miami Blvd., Durham NC, 27703 USA*
(email: russell.harmon@us.army.mil)
[4] *U.S. Army Research Laboratory, Aberdeen Proving Ground, MD, 21005 USA*

ABSTRACT: In this study, statistical classification techniques have been applied to LIBS data for a large suite of garnets of different composition from different places around the world. Each broadband LIBS spectrum contains measured light intensities between 200 and 880 nm collected over 13,600 channels in a CCD spectrometer. The Matlab® program was used to perform a high-dimensional principal components analysis (HDPCA) on the data set. Individual garnet LIBS spectra were grouped according to the similarities in the linear combination of their principal components. Because of the large volume of data and the ability of Matlab® to display results in multiple dimensions, an accurate model could be created that was able to successfully classify unknown garnet samples of a specific composition type according to their geographic origin.

KEYWORDS: *Laser-induced breakdown spectroscopy, garnet, LIBS, multivariate principal components analysis, geochemical fingerprinting*

INTRODUCTION

The ability to geographically identify the source area of natural gems plays an important role in determining if these stones may have originated from a politically unstable area. Garnet is a semi-precious silicate mineral of variable composition that has been used as a gemstone since the Bronze Age.

In LIBS, a pulsed laser beam is focused on a sample such that energy absorption produces a high-temperature microplasma at the sample surface. Small amounts (nanograms) of material are dissociated and ionized, with both continuum and atomic/ionic emission generated by the plasma during cooling. A broadband spectrometer-detector is used to spectrally- and temporally-resolve the light from the plasma and record the intensity of elemental emission lines. Since the technique is simultaneously sensitive to all elements, a single laser shot can be used to record the broadband LIBS emission spectra, which are unique chemical 'fingerprints' of a material.

BACKGROUND

The garnet group of minerals can be described by the general compositional formula $A_3B_2(SiO_4)_3$, where A and B refer respectively to cation sites 8-fold and 6-fold coordination. The A sites are occupied by rather large divalent cations, whereas the B sites host smaller trivalent cations. Garnets occur in many different geologic settings, which typically determine the particular species of garnet present. The six common species of garnet comprise two groups on the basis of their ideal end-member chemical compositions as follows: The Pyralspite Garnet Group consists of Almandine $[Fe_3Al_2(SiO_4)_3]$, Pyrope $[Mg_3Al_2(SiO_4)_3]$, and Spessartine $[Mn_3Al_2(SiO_4)_3]$ whereas the Ugrandite Garnet Group comprises Andradite $[Ca_3Fe_2(SiO_4)_3]$, Grossular $[Ca_3Al_2(SiO_4)_3]$, and Uvarovite $[Ca_3Cr_2(SiO_4)_3]$. Six other minor species of garnet occur in nature, but are not common.

RESULTS

In this study, we acquired broadband LIBS spectra at the Army Research Laboratory for more than 125 garnet samples from 76 different locations worldwide. Sets of 25 single laser shot broadband spectra were for 28 spessartines, 37 andradites, 32 grossulars, 12 pyropes, 26 almiandines, and 10 uvarovites. The resultant garnet LIBS spectral database was analyzed by multivariate statistical analysis after averaging the LIBS spectra for each sample.

Broadband LIBS spectra for three garnet types – the Mg-Al pyrope type, the Ca-Al grossular type, and the Mn-Al spessartine type are shown in Figure 1.

The high dimensional nature of LIBS signals can lead to several computational issues when used in conjunction with many machine learning techniques. Dimensionality reduction is the process by which the high dimensional signals are mapped into a lower dimensional space. The resulting lower dimensional space can enable more robust performance when used in conjunction with pattern recognition techniques.

Principal components analysis (PCA) is a standard technique for dimensionality reduction that finds a linear mapping from the high dimensional space to a lower dimension space. The linear mapping is chosen to maximize the variance in the resulting lower dimensional space and is determined by performing an Eigen-decomposition on the covariance matrix of the observation dimensions. Due to memory limitations, the required covariance matrix cannot be calculated when the number of observation dimensions is extremely large, as is the case with LIBS signals. This work utilizes an alternate formulation of PCA that is applicable to datasets with high dimensional observations, high dimensional PCA (HDPCA) (Bishop, 2007). HDPCA calculates the covariance matrix of the observations instead of the observation dimensions. Therefore, for data sets containing fewer observations than observation dimensions, such as LIBS signals, HDPCA provides a tractable method for performing dimensionality reduction.

The results of the HDPCA analysis for the 4 groups of spessartine garnets from locations in Australia, China, Brazil, and Virginia are shown in Figures 2 and 3. The K-nearest-neighbour analysis (K=5, in two dimensions, 2nd and 3rd) results in a 93.3% correct sample classification (Fig. 2). The shaded areas corresponding to the symbols in the legend are the areas most likely to find an unknown sample from that region. By comparison, the results of the 'leave-one-out' classification analysis shown in Figure 3 results in a slightly higher classification success at 94.6%. Figure 4 shows the classification

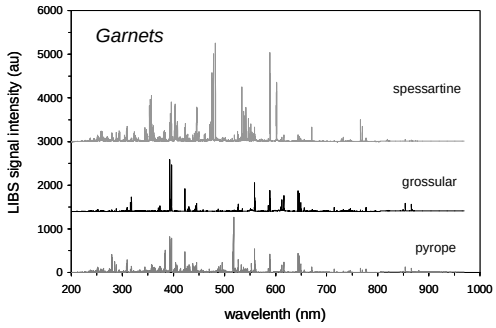

Fig.1. Example broadband LIBS spectra for a pyrope, grossular, and spessartine garnet. The clear differences observed in the broadband spectra reflect the chemical differences in the composition of the three garnets.

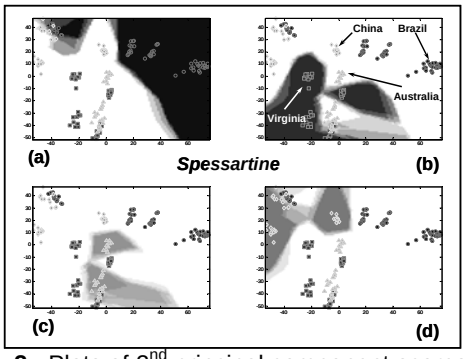

Fig. 2. Plots of 2nd principal component scores (x-axis) verses 3rd principal component scores (y-axis) showing the regions of space where unknown spessartine data points would be classified as originating from one of the four geographic locations: Brazil, Virginia, Australia, and China, clockwise form upper right, respectfully.

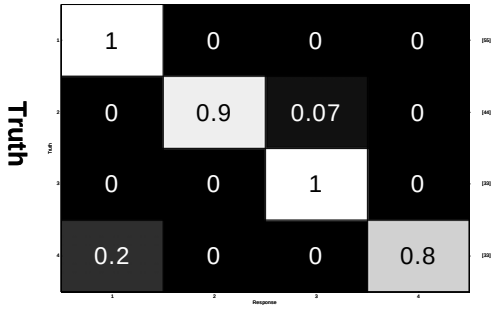

Fig. 3. Confusion matrix for the HDPCA analysis of four spessartine garnets from different locations worldwide. The nth row and column correspond to the nth spessartine type truth and HDPCA statistical assignment, respectively.

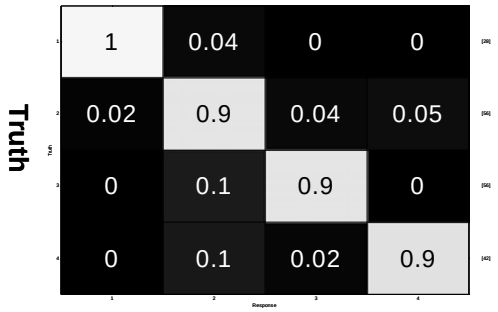

Fig. 4. Confusion matrix for the HDPCA analysis of the four pyrope garnets. The nth row and column correspond to the nth pyrope type truth and HDPCS statistical assignment, respectively.

confusion matrix for four groups of pyrope garnet from North Carolina, the Kimberly area of South Africa, Arizona, and Bohemia, in the Czech Republic. Figure 5 shows the confusion matrix for four groups of grossular garnet from the Inyo City area of California, Vermont, the Asbestos area of Quebec in Canada, and the Coaluila area of Mexico.

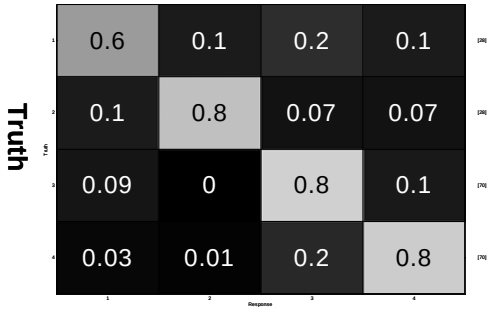

Fig. 5. Confusion matrix for the HDPCA analysis of the four grossular garnets. The nth row and column correspond to the nth grossular type truth and HDPCS statistical assignment, respectively.

CONCLUSIONS

Important attributes of a LIBS sensor system for geochemical analysis include (i) real-time response, (ii) in-situ analysis with no sample preparation required; (iii) a high sensitivity to low atomic weight elements which are often difficult to determine by other techniques, and (iv) standoff detection. LIBS technology is now sufficiently mature, inherently rugged, and affordable to offer a capability for both laboratory and field-deployable analysis. A successful laboratory benchtop feasibility study of garnets has been conducted that highlights the potential of LIBS for mineralogical identification and classification.

REFERENCES

BISHOP, C.M. 2007. Pattern Recognition and Machine Learning, Springer.

The U-tube sampling methodology and real-time analysis of geofluids

Barry Freifeld[1], Ernie Perkins[2], James Underschultz[3], & Chris Boreham[4]
[1]*Lawrence Berkeley National Laboratory, Berkeley, CA USA (bmfreifeld@lbl.gov)*
[2]*Alberta Research Council, Edmonton, AB CANADA*
[3]*CSIRO Petroleum & CO2CRC, Bentley, WA AUSTRALIA*
[4]Geoscience Australia & CO2CRC, Canberra, ACT *AUSTRALIA*

ABSTRACT: The U-tube geochemical sampling methodology, an extension of the porous cup technique proposed by Wood (1973), provides minimally contaminated aliquots of multiphase fluids from deep reservoirs and allows for accurate determination of dissolved gas composition. The initial deployment of the U-tube during the Frio Brine Pilot CO_2 storage experiment, Liberty County, Texas, obtained representative samples of brine and supercritical CO_2 from a depth of 1.5 km. A quadrupole mass spectrometer provided real-time analysis of dissolved gas composition. Since the initial demonstration, the U-tube has been deployed for (1) sampling of fluids down gradient of the proposed Yucca Mountain High-Level Waste Repository, Armagosa Valley, Nevada (2) acquiring fluid samples beneath permafrost in Nunuvut Territory, Canada, and (3) at a CO_2 storage demonstration project within a depleted gas reservoir, Otway Basin, Victoria, Australia. The addition of in-line high-pressure pH and EC sensors allows for continuous monitoring of fluid during sample collection. Difficulties have arisen during U-tube sampling, such as blockage of sample lines from naturally occurring waxes or from freezing conditions; however, workarounds such as solvent flushing or heating have been used to address these problems. The U-tube methodology has proven to be robust, and with careful consideration of the constraints and limitations, can provide high quality geochemical samples.

KEYWORDS: *geochemical sampling, carbon sequestration, borehole sampling, fluid sampling*

INTRODUCTION

Obtaining uncontaminated fluid samples from deep geologic aquifers is challenging because of the elevated pressures and temperatures encountered. Entering wellbores that are under pressure and which may contain explosive or sour gas is a complex task that requires the deployment of well-head pressure control equipment along with cranes or workover rigs to utilise wireline conveyed samplers. The technology to maintain fluid sample integrity during recovery has been developed primarily within the oilfield and geothermal service industries, with examples of commercially available instruments being: Schlumberger's MDT fluid sampler; Halliburton's Armada Sampling System; and Kuster Corporation's flow through sampler. All three of these sampling devices are mechanically complex and need to be conveyed into and out of a wellbore to facilitate each sample recovery.

The U-tube was developed to simplify the recovery of fluids from deep boreholes and allow flexibility for post-sampling analysis (Freifeld *et al*. 2005; Freifeld & Trautz 2006). In particular, the ability to repeatedly collect large volume multiphase samples into high pressure cylinders facilitates both real-time field analysis as well as acquisition of sample splits for future laboratory based analysis.

U-TUBE OPERATION

The U-tube is permanently or semi-permanently deployed in a wellbore to provide the ability to periodically (or continuously) acquire samples. The U-tube is extremely simple, consisting of a loop of tubing, which has a tee at its base, terminating at a check valve that permits fluid to enter the loop of tubing (Fig. 1). A filter at the inlet removes particulates that can interfere with the operation of the check valve. At the surface, the U-tube drive leg is connected to a supply of high pressure N_2 that closes the check valve

Fig. 1. Schematic layout of the downhole equipment for deploying a U-tube geochemical sampler.

and forces the sample that collects within the loop of tubing up the sample leg to the surface.

In its most basic form the surface sampling equipment can consist of an open container at which the sample leg terminates. However, for higher purity sampling or accurate dissolved gas chemistry analysis, the sample is directed into N_2 purged and/or evacuated high pressure sample cylinders. After a sample has been acquired, by venting both the sample and drive legs to atmospheric pressure, the check valve is allowed to open and fresh sample enters the U-tube sampling loop.

U-TUBE DEPLOYMENT

To date, we have deployed the U-tube using several distinct modalities depending on the wellbore completion requirements. As part of Nye County's Nuclear Waste Repository Early Warning groundwater monitoring program, a borehole in the Armagosa Valley, Nevada, USA, was completed with four U-tubes within two sand packs. At depths of 265 m and 350 m, two U-tubes were located within each sandpack and isolated using a bentonite backfill.

At the High Lake Site in Nunuvut Territory, Canada, a 7.5 cm diameter mineral exploration boring was completed with a U-tube to sample sub-permafrost brines (Freifeld *et al*. 2008). Small gage (1/4") stainless steel tubing served as the drive and sample legs of the U-tube as well as functioned as the strength member for lowering the U-tube and pneumatic packer to a depth of ~400 m. To prevent freezing within the sampling lines a heat trace providing 20 W/m was run along the entire length of the borehole completion.

As part of geologic CO_2 sequestration demonstration projects conducted at the Frio Site, Liberty County, TX, USA, and the Otway Project, Nirranda South, Victoria, Australia, U-tubes were deployed for sampling multi-phase mixtures of gas, water and supercritical CO_2. At both these sites, CO_2 was injected in the subsurface to understand the subsurface movement of the CO_2 plume and geochemical sampling was one of many technologies employed to understand the fate of the CO_2.

SAMPLE ACQUISITION & ANALYSIS

The method for U-tube sample retrieval is determined by the end use of the collected fluid. For the relatively shallow fluid collection at Nye County's Amargosa Valley Site and at the High Lake Site, samples were driven to the surface using compressed N2 gas supplied in standard 'G' size (~8000 l) industrial cylinders. At both the Amargosa and High Lake site, samples were collected at 1 bar and there was no attempt to maintain sterile sampling conditions.

For the CO2 sequestration programs at the Frio Field Site and the Otway Project, samples were collected in high pressure, large volume (13 l) cylinders for surface processing. To maintain sample integrity the pressure cylinders at the Frio Site were flushed with N2 and then evacuated using a rotary vane pump prior to filling to formation pressure with fluid from the U-tubes.

Because of difficulty in keeping vacuum pumps operating when they are exposed to significant volumes of moisture laden gas, it was decided that after flushing the sample cylinders with N2, they would be allowed to bleed down to 1 bar pressure but not evacuated. The residual 13 l of N2 in the sample cylinders acted as an internal standard, enabling an accurate estimation of dissolved gas concentration in the sample fluid (Freifeld & Trautz 2006).

FRIO FIELD SITE

At the Frio Field Site, because of the need for real-time feedback to guide operational decision making and the ephemeral nature of some of the monitored parameters, significant effort was given toward field analysis. To measure the pH before degassing, a high pressure pH electrode (Model TB567, ABB Inc. Reno, Nevada, USA) was installed on the high pressure sample line. In addition, benchtop measurements were acquired of electrical conductance, pH and alkalinity soon after sample collection (Kharaka *et al.* 2006).

A field deployable quadrupole mass spectrometer (Omnistar, Pfiffer Vaccuum GmbH, Asslar, Germany) was used to detect the arrival of the CO_2 plume in addition to determine CH_4 , O_2, Ar and N_2 concentrations. Various tracers including Kr, SF_6 and perfluorocarbons were periodically co-injected with CO_2 to aid in determining rates of subsurface transport and changes in CO_2 saturation (Freifeld *et al*. 2005). The gas tracers can be determined to a precision of ±100 ppb or better using the mass spectrometer, although frequent calibration is required to obtain this level of accuracy.

OTWAY PROJECT

The Otway Project is using a multilevel completion with three U-tubes to sample above and below the gas-water contact of a depleted gas reservoir, while CO_2 is injected in a well located 300 meters downdip. The uppermost U-tube was installed just below the mudstone cap rock and is sampling predominantly supercritical CH_4, while the lower two U-tubes initially produced water, but transitioned to predominantly CO_2 and CH_4 as the gas-water contact was pushed down by the increasing volumes of CO_2.

Early in the sampling program it was observed that there was a decrease in gas flow from the sample leg for the U-tube accessing the residual gas column. This flow restriction was found to be caused by a progressive build-up of wax within the ¼" sample line at the near surface. The wax composition was dominated by a homologous series of n-alkanes, maximizing at n-C_{27}, with a melting point of ~41^{o}C; a temperature that would cause it to solidify during surface sampling. Following a solubility study of different commercially available solvents, a product sold by ExxonMobil under the trade name Solvesso-100, composed primarily of $C_{9\text{-}10}$ dialkyl and trialkylbenzenes, provided the best solution for periodic flushing of wax that collects within the U-tube sampling lines.

Figure 2 shows the molar fraction of CO_2 in the samples for all three U-tubes. Initial small increases in CO_2 appear in July for U-tube 2 (3 ½ months after the

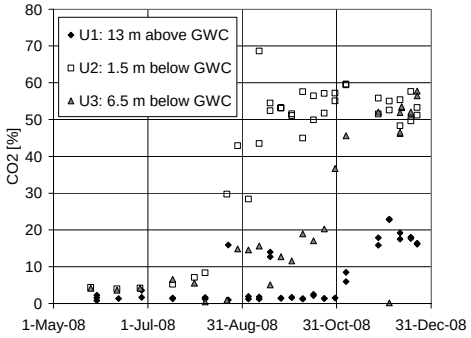

Fig. 2. Molar fraction of CO2 in gas samples collected in U-tubes at the Otway Project.

start of CO2 injection), and August for U-tube 3. After the initial appearance as a dissolved phase, the CO_2 molar fraction rapidly increases as a free-phase gas component arrives. U-tube 2 became self lifting in September and no further water samples were obtained. Similarly for U-tube 3 the transition to gas occurred at the very end of December 2008, with the samples collected in 2009 containing only small amounts of liquid.

CONCLUSIONS

The U-tube geochemical sampling system has been demonstrated to operate in varied environmental conditions, from direct burial in sand/bentonite backfill to deep oil and gas reservoirs. As with all borehole sampling methods, careful attention needs to be paid to the type of fluid being sampled, the purpose of the sampling and the interaction of the borehole with the surrounding formation. By addressing potential sampling difficulties and carefully controlling wellbore conditions, U-tubes can provide high purity samples for real-time and laboratory analysis.

ACKNOWLEDGEMENTS

This work was supported by the Assistant Secretary of the Office of Fossil Energy, U.S. Department of Energy, National Energy Technology Laboratory under contract DE-AC03-76SF00098. The CO2CRC Otway Project is funded by Australian Federal and State governments and industrial and academic partners in Australia and abroad.

REFERENCES

FREIFELD, B.M. & TRAUTZ, R.C. 2006. Real-time quadrupole mass spectrometer analysis of gas in borehole fluid samples acquired using the U-tube sampling methodology. *Geofluids,* **6**, 217–224. doi: 10.1111/j.1468-8123.2006.00138.x.

FREIFELD, B.M., TRAUTZ, R.C., YOUSIF K.K., PHELPS, T.J., MYER, L.R., HOVORKA, S.D., & COLLINS, D. 2005. The U-Tube: A novel system for acquiring borehole fluid samples from a deep geologic CO_2 sequestration experiment. *Journal Geophysical Research,* **110**, B10203, doi:10.1029/2005JB003735.

FREIFELD, B.M ., FINSTERLE, S., ONSTOTT, T.C., TOOLE, P., & PRATT, L.M. 2008. Ground surface temperature reconstructions: using in situ estimates for thermal conductivity acquired with a fiber-optic distributed thermal perturbation sensor. *Geophysical Research Letters,* **35**, L14309, doi:10.1029/2008GL034762.

KHARAKA Y.K., COLE D.R., HOVORKA S.D., GUNTER W.D., KNAUSS K.G., & FREIFELD, B.M. 2006. Gas-water-rock interactions in Frio Formation following CO_2 injection: Implications for the storage of greenhouse gases in sedimentary basins. *Geology*, **34**, 577–580.

WOOD, W. 1973. A technique using porous cups for water sampling at any depth in the unsaturated zone. *Water Resources Research*, **9**, 486–488.

LIBS as an archaeological tool – example from Coso Volcanic Field, CA

Jennifer L. Gottfried [1], Russell S. Harmon[2], Anne Draucker[3], Dirk Baron[3], & Robert M. Yohe[3]

[1]*U.S. Army Research Laboratory, Aberdeen Proving Ground, MD, 21005 USA*
[2]*ARL Army Research Office, 4300 S. Miami Blvd., Durham NC, 27703 USA*
(email: russell.harmon@us.army.mil)
[3]*Department of Physics and Geology, California State University, Bakersfield, Bakersfield, CA, 93311 USA*

ABSTRACT: Recently, multi-element chemical analysis of has become a common means for attributing the provenance of archaeological materials. Laser-induced breakdown spectroscopy (LIBS) is a simple atomic emission spectroscopy technique with potential for real-time man-portable chemical analysis in the field. Because LIBS is simultaneously sensitive to all elements, a single laser shot can be used to record the broadband emission spectra, which provides a 'chemical fingerprint' of a material. Sets of single-shot broadband LIBS spectra were collected for a suite of 27 obsidians from major sites across the Coso Volcanic Field (CVF), as well as for samples from 4 other California obsidian locations – Bodie Hills, Mt. Hicks, Fish Springs, and Shoshone. Different advanced statistical signal processing techniques were applied to the obsidian data. Although all obsidian samples exhibited quite similar broadband LIBS spectra, the 5 different California obsidian locations could be clearly discriminated. Within the CVF, it is possible to distinguish the five sub-groupings defined on the basis of previous ICP-MS analysis. Samples from the Joshua Ridge are a distinct group, those from the S, SE, and W Sugarloaf locations are strongly correlated, as are samples from the Cactus Peak and E Sugarloaf and the West Cactus Peak and Stewart locations.

KEYWORDS: *Laser-induced breakdown spectroscopy, LIBS, multivariate spectral analysis, obsidian sourcing, geochemical fingerprinting*

INTRODUCTION

Obsidian is a naturally occurring volcanic glass that has long been used by ancient peoples as a raw material for producing tools. Hydration dating and geochemical studies of obsidian can provide archaeologists with important means of understanding artifact production and past trade patterns (Erickson 1981). In particular, multi-element chemical analysis of obsidian has become an accepted procedure for attributing the provenance of artifacts, particularly obsidian (e.g. Shackley 2005; Negash *et al*. 2006).

GEOLOGICAL SETTING

The Coso Volcanic Field (CVF) in California, USA (Fig. 1) contains at least 38 high-silica rhyolite domes (Duffield & Bacon 1981), many of which contain obsidian glass that has been quarried for tools by the indigenous population for more than 12,000 years. CVF obsidian artifacts are found throughout southwestern USA and sourcing of CVF obsidian for archaeological studies by geochemistry has been an important tool in assessing prehistoric trading patterns across the Great Basin (Gilreath & Hildebrandt 1997).

The obsidians of the CVF are crystal-

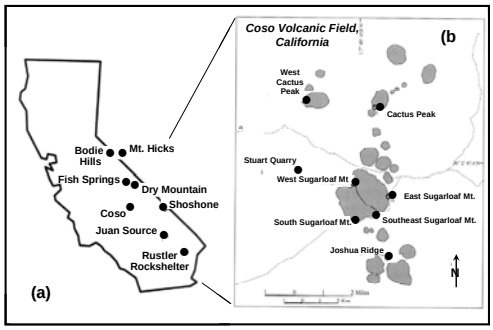

Fig. 1. (a) California map showing the obsidian sources analyzed and (b) map of the Coso Volcanic Field (after Duffield & Bacon 1981; Hughes 1988)

poor, high-silica, metaluminous rhyolites that containing 77±0.6% SiO_2 (Bacon *et al.* 1981) that are similar to rhyolites found in California and western Nevada, such as those present at Mt. Hicks, Bodie Hills, Fish Springs, and Shoshone (Fig. 1).

Geochemical studies by Hughes (1988), Ericson & Glascock (2004), and Drucker (2007) employing multivariate statistical analysis have delineated major obsidian sub-sources within the CVF. This study was undertaken to ascertain the extent which LIBS could be applied to the problem of obsidian sourcing through analysis of the same suite of samples that was analyzed by Draucker (2007).

RESULTS

The emerging analytical technique of laser-induced breakdown spectroscopy (LIBS) is a simple atomic emission spectroscopy technique that has the potential for real-time man-portable chemical analysis in the field. Because LIBS is simultaneously sensitive to all elements, a single laser shot can be used to record the broadband emission spectra, which provides a 'chemical fingerprint' of a material.

We collected sets of single-shot broadband LIBS spectra in the Army Research LIBS Laboratory for 27 obsidian samples from major sites across the CVF as well as for samples from 4 other California obsidian locations – Bodie Hills, Mt. Hicks, Fish Springs, and Shoshone. The resultant obsidian LIBS spectral database was analyzed by multivariate statistical analysis.

A total of 185 emission lines for both major and trace elements were attributed from each LIBS broadband spectrum. Then background-corrected, summed, and normalized intensities were calculated for 18 selected emission lines and 153 emission line ratios were generated. Finally, the summed intensities and ratios were used as input variables to multivariate statistical chemometric models. A total of 3100 spectra were used to generate Partial Least Squares Discriminant Analysis (PLS-DA) models and test sets.

A model was built for discriminating the five distinct obsidian localities (Coso, Mt. Hicks, Fish Springs, Shoshone, and Bodie Hills), the broadband LIBS spectra for which exhibit a high degree of visual similarity; 100% of the 200 test single-shot spectra were correctly classified with that model (Table 1). In other words, obsidian samples from the 5 regions are easily distinguishable with LIBS.

When the 575 remaining Coso spectra (from samples not used in the 5-class model) were tested against the model, 574 out of 575 were correctly classified with the other Coso samples in the model. In other words, the model remains valid even for unknown samples (Table 2).

Subsequently, a more complex PLS-DA model (not shown) was built based on individual classes for each of the 31 obsidian samples in order to identify similarities between samples from different geographical areas. From these results, it was concluded that the South, SE, and West Sugarloaf samples are strongly correlated with each other, as are the Cactus Peak and East Sugarloaf and the West Cactus Peak and Stewart samples. The Cactus Peak, West Cactus, E Sugarloaf and Stewart samples also have similar LIBS features.

CONCLUSIONS

Although all obsidian samples exhibited quite similar broadband LIBS spectra, the PLS-DA approach was able to clearly discriminate samples from the 5 different California obsidian locations. Within CVF, it is possible to distinguish the five sub-groupings defined on the basis of ICP-MS

Table 1. Confusion matrix for the PLS-DA analysis of the California obsidian localities using 600 broadband LIBS spectra and 15 latent variables to produce 5 model classes. Horizontal lines separate the groupings for the Coso Volcanic Field by Draucker (2007) and the other four California obsidian localities

		Model Classes					
Test Samples		165 179 186 176	164	172	173	174
Joshua Ridge (B-J)	165	25	0	0	0	0
E Sugerloaf (B)	179	25	0	0	0	0
SE Sugarloaf (2-L)	186	25	0	0	0	0
South Stewart (L)	176	25	0	0	0	0
Mt Hicks	164	0	25	0	0	0
Fish Springs (Inyo)	172	0	0	25	0	0
Shoshone	173	0	0	0	25	0
Bodie Hills	174	0	0	0	0	25

Table 2. Confusion matrix for a test of the PLS-DA model for the Coso obsidian locality. The remaining 575 broadband LIBS spectra for Coso (not included in the original model) were assigned with nearly perfect locality classification (99.8%). Only Coso sample #189 from South Sugarloaf had some misclassification with Shoshone sample #173.

.

		Model Classes						
'Unknown' Test Samples		165	179	186	176	164	172	173	174
Joshua Ridge (O)	166	25				0	0	0	0
Cactus Peak (2-T)	167	25				0	0	0	0
Cactus Peak (1-J)	168	25				0	0	0	0
Cactus Peak (1-L)	169	25				0	0	0	0
E Sugerloaf (D)	180	25				0	0	0	0
E Sugerloaf (E)	181	25				0	0	0	0
SE Sugarloaf (1-O)	183	25				0	0	0	0
SE Sugarloaf (1-V)	184	25				0	0	0	0
SE Sugarloaf (2-F)	185	25				0	0	0	0
S Sugarloaf (1-L)	182	25				0	0	0	0
S Sugarloaf (3b-I)	187	25				0	0	0	0
S Sugarloaf (2-L)	188	25				0	0	0	0
S Sugarloaf (3a-N)	189	24				0	0	4	0
W Sugarloaf (1-O)	190	25				0	0	0	0
W Sugarloaf (2-R)	191	25				0	0	0	0
W Sugarloaf (3-I)	192	25				0	0	0	0
W Sugarloaf (4-M)	193	25				0	0	0	0
West Cactus (B)	170	25				0	0	0	0
West Cactus (A)	171	25				0	0	0	0
South Stewart (M)	175 (large)	25				0	0	0	0
South Stewart (M)	175 (small)	25				0	0	0	0
South Stewart (K)	177	25				0	0	0	0
North Stewart (J)	178	25				0	0	0	0

analysis. Samples from the Joshua Ridge are a distinct group, those from the S, SE, and W Sugarloaf locations are strongly correlated, as are samples from the Cactus Peak and E Sugarloaf and the West Cactus Peak and Stewart locations.

REFERENCES

BACON, C.R., MACDONALD, R., SMITH, R.L., & Baedecker, P.A. 1981. Pleistocene high-silica rhyolites of the Coso Volcanic Field, Inyo County, California. *Journal of Geophysical Research,* **86**, 10223-10241.

DRAUCKER, A.C. 2007. *Geochemical characterization of obsidian subsources from the Coso Range, California using laser ablation inductively coupled plasma mass spectrometry as a tool for archaeological investigations.* MS thesis, California State University at Bakersfield, Bakersfield, California.

DUFFIELD, W.A. & BACON, C.R. 1981. Geologic map of the Coso Volcanic Field and adjacent areas, Inyo County, California. *U.S. Geological Survey Miscellaneous Investigations* **Map I-1200**.

ERICKSON, J.E. 1981. Exchange and production systems in Californian prehistory: The results of hydration dating and chemical characterization of obsidian sources. *British Archaeological Reports International Series*, **110**, 1-240.

ERICKSON J.E. & GLASCOCK, M.D. 2004. Subsource Characterization: Obsidian utilization of subsources of the Coso Volcanic Field, Coso Junction, California, USA. *Geoarchaeology,* **19**, 779-805.

GILREATH, A.J. & HILDEBRANDT, W.R. 1997. Pregistoric use of the Coso Volcanic Field. *Contributions of the University of California Archaeological Research Facility.*

HUGHES, R.E. 1988. The Coso Volcanic Field Reexamined: Implications for obsidian sourcing and hydration dating research. *Geoarchaeology*, **3**, 253-265.

NEGASH, A., SHACKLEY, M.S., & ALEVE, M. 2006. Source provenance of obsidian artifacts from Early Stone Age (ESA) site of Melka Konture, Ethiopia, *Journal Archaeological Science,* **33**, 1647-1650.

SHACKLEY, M.S. 2005. Obsidian -Geology and archaeology in the North American Southwest. *University of Arizona Press*.

The application of visible/infrared spectrometry (VIRS) in economic geology research: Potential, pitfalls and practical procedures

Andrew Kerr, Heather Rafuse, Greg Sparkes, John Hinchey, & Hamish Sandeman

Geological Survey of Newfoundland and Labrador, Department of Natural Resources, PO Box 8700, St. John's, NL, A1B 4J6. CANADA (e-mail: andykerr@gov.nl.ca)

ABSTRACT: Portable visible/infrared spectroscopy (VIRS) instruments now have wide application in mineral exploration, exploitation, processing, environmental monitoring and numerous other fields that require characterization of natural and artificial materials. This method utilizes the absorption response of many minerals to electromagnetic radiation in the visible, near infrared and shortwave infrared regions, i.e., from about 350 nm to 2500 nm. Data can be acquired rapidly, and can provide very useful insights, notably with respect to hydrothermal alteration assemblages, which include many minerals with distinctive VIRS patterns. Despite its great potential, there is presently limited published information due to confidentiality issues, and the use of VIRS in research-oriented studies is less common. Our experience since acquiring a VIRS instrument in 2008 has convinced us of its great potential, but results from pilot studies show that the acquisition and interpretation of data is not always simple and direct. There is a need for a collaborative effort to develop and publish procedures, protocols and libraries for such studies; this initiative would facilitate greater use of these methods as standard tools for research in economic geology and other aspects of Earth Sciences.

KEYWORDS: *visible/infrared spectrometry, economic geology, alteration, mineralization*

INTRODUCTION

Over the last 10 years, portable infrared and visible/infrared optical spectrometers have become common tools for both mineral exploration purposes and also in operating mines. These instruments have great potential for the characterization of natural materials in a variety of fields related to environmental science, earth science and archaeology. The most obvious geoscience application is towards understanding hydrothermal alteration in mineralizing systems, and this is the main objective where such instruments are used in exploration (e.g., Thompson *et al.* 1996). Mapping of alteration is critically important as an exploration tool and also as a route to understanding the genesis of mineral deposits, and it follows that VIRS instruments should be widely applicable to economic geology research by both government agencies and academic institutions. The portability of such instruments lends itself to direct application in the field, although the Newfoundland climate has to date discouraged us from taking our instrument out on traverses.

Despite this obvious potential, there are very few published sources providing case studies or guidelines for data acquisition, processing and interpretation. This absence undoubtedly reflects the proprietary and confidential nature of results obtained in exploration programs.

The Geological Survey of Newfoundland and Labrador (GSNL) acquired a Terraspec Pro™ VIRS spectrometer in 2008, and we are currently applying it in several research projects related to diverse styles of mineralization, and also as a practical aid to local prospectors and companies interested in identifying minerals and alteration facies. These studies are to some extent pilot projects, and are linked to the development of methodology and protocols for acquiring and interpreting the data from both empirical and mineralogical perspectives. The results illustrate the great potential of

VIRS methods as pragmatic and scientific tools, but they also point to some of the complications that can influence and in some cases compromise results. This presentation is intended to share some of our experiences in using this remarkable technology, and also to initiate discussion of various ideas that could lead to greater sharing of information amongst research institutions using VIRS instruments.

BACKGROUND AND TECHNICAL ASPECTS OF VIRS ANALYSIS

VIRS is to a large extent an outgrowth of the space exploration programs of the last 50 years, in which there was a need to develop methods for the remote imaging of the Earth and other planets. The method depends on a well-known phenomenon, ie., the response of natural materials to electromagnetic radiation. The colour of common minerals results from differential absorption of specific visible wavelengths, although there is only rarely a simple relationship between colour and composition. However, a very large number of minerals have distinct wavelength-specific absorption in the near Infrared (NIR) and short-wave infra red (SWIR) regions of the spectrum. Not all such absorption features are unique to a given mineral, but a combination of such features can be very diagnostic, and may also yield qualitative information about compositional parameters.

Not all minerals are active in the infrared and the common anhydrous rock-forming silicates (e.g., quartz, feldspars, pyroxenes, etc.) are generally unresponsive. This may seem at first sight to be a disadvantage, but it has a good side also, in that it allows the recognition of important alteration minerals in small proportions, often below the threshold of visual identification. Spectra obtained from rocks containing several infrared active species represent mixtures, but they are not necessarily linear mixtures of individual spectra, as minerals vary in their reflectance. The interpretation of data from mixed assemblages is perhaps the greatest challenge in using VIRS instruments as research tools, and it is almost unavoidable.

SPECTROMETER OPERATION AND DATA COLLECTION ASPECTS

The spectrometer itself has a relatively simple design, although it is of course complex in its details. A specialized light source within a “probe” irradiates the sample, and reflected light is transmitted into the analytical module by a fibre-optic cable. Three separate spectrometers analyze the response at wavelengths from 350 nm to 2500 nm, and provide digital input to the control system, which is a customized laptop computer. The acquisition of data is very rapid – once the machine is initiated and calibrated, individual spectral measurements take less than 60 seconds. The retention and recording of key information about the location and geological context of the measurement is a significant concern, and careful record-keeping is vital. The use of digital photographs of the sample, upon which the locations of individual measurements can be directly plotted and numbered, is one of the methods that we have adopted.

ISSUES IN DATA PROCESSING AND INTERPRETATION

The results from VIRS analyses are amenable to several methods of interpretation. In the simplest sense, the spectra can be used as empirical measurements on given rock types or formations, without specific reference to the causative minerals. We have found that superficially identical rock types with different geological contexts can in some cases be effectively characterized and discriminated. The comparison of measured spectra with reference spectra from minerals is the main tool used for identification, and is very effective in cases where samples are monomineralic or dominated by a single infrared active species. The size of the area analyzed is ~ 1 cm in diameter. Computer programs with variable levels of automation can speed the process of identification, but

they need to be used with a measure of caution where spectra are likely to have mixed sources. Our experience is that human observation and reasoning is important if the maximum amount of information is to be gleaned from a dataset.

Some basic data processing is required once the data are acquired. These include "splicing" (to remove small offsets related to the use of three discrete detection systems for different wavelength ranges) and also averaging of individual measurements where appropriate. Our experience is that homogeneous samples produce identical spectra from several measurements, although their total amplitude may vary. These data can be reduced by numerical averaging, although individual spectra must first be closely examined, to be sure that they do not contain a distinct response recording the heterogeneous distribution of some key mineral.

The amount of reflectance from a sample is influenced by factors such as colour and also the nature of the surface. Surprisingly, smooth surfaces such as cut drill core provide lower amplitude spectra than rough or uneven surfaces such as broken core or hand samples. However, the geometry of spectra (ie., the presence of discrete absorption features) is retained even when overall reflectance is reduced. The comparison of measured spectra with reference spectra is hampered by such differences in amplitude, and we have found it advantageous to "normalize" spectra such that all results have the same overall apparent range in reflectance. This is a simple scaling procedure once the maximum and minimum values are obtained, and is easily performed using instrument software or standard spreadsheet programs. It can also be carried out in a more qualitative manner after the results are imported into graphics programs for display.

Dealing with spectral responses from samples that contain mixed assemblages is a significant challenge. If one of the alteration minerals is highly reflective, its response may drown out that from other species that may also be important. An example of this is provided by results from a VMS alteration zone, in which kaolinite group minerals were independently identified by XRD. In the VIRS data, the response from these species was generally overcome by a strong response from "sericite" (i.e., hydrous muscovites and related minerals). Our experience is that a valuable first step is to seek responses from areas where a single mineral species is dominant; this allows the identification of the "end members" that will contribute to a composite spectrum. These measurements can then be used as input in attempts to broadly quantify the proportions of minerals in mixtures and the progressive development of alteration "facies".

CASE STUDIES

In our initial use of VIRS methods, we have chosen a diverse set of projects. These include epithermal-style precious metal mineralization (eastern and central Newfoundland), mesothermal gold mineralization (Central Newfoundland), syngenetic VMS mineralization and related alteration (Central Newfoundland), porphyry-style Mo-Cu mineralization (southern Newfoundland) and uranium mineralization in the Central Mineral Belt of Labrador. Space does not permit detailed discussion of results, but in all cases we were able to recognize distinctive alteration species and document their distribution. In some cases, results provided surprises, eg., the recognition of topaz in quartz-alunite alteration and possible Li-rich micas in VMS alteration influenced by magmatic fluids. In some cases, the resolution of species in mixed assemblages proved to be difficult, but the overall spectral patterns could still be used to discriminate alteration facies and demonstrate their superposition.

Using these techniques has not proved as simple as we might have hoped, but this should come as no surprise given the innovative nature of the technology and the complexity of natural systems. The

methods have great untested potential as research tools, but like any analytical technique, they acquire greater power and significance when they can be linked to other types of independent information, such as lithogeochemical data, petrographic analysis and XRD measurements.

WHERE SHOULD WE GO FROM HERE?

The successful use of VIRS methods as research tools requires more than anything a published framework that will provide standards for the collection and interpretation of data, and accessible data libraries that can give examples for comparison and contrast. The spectral libraries used for mineral identification are in part public-domain, but much information remains tied to the instrument software and cannot readily be distributed. Differences in the formats used for spectral files in different libraries complicate their use in standard software and impedes information exchange.

The development of spectral reference libraries geared to specific mineralizing environments or geographic regions (eg., VMS deposits in eastern Canada, or Cordilleran Mo-W deposits) would be a very useful step, especially if such resources were available through a single integrated website. Such reference spectra should not be restricted to individual minerals (although these are important) but should include information from real rocks that contain mixed assemblages and have known geological and metallogenic contexts. Dealing with mixed responses is an almost unavoidable problem in most situations that we can envisage.

There may also be a need for "standards" that can be used to calibrate instruments, check for progressive shifts in their measurement responses, and ensure that data acquired from different sources are comparable. In most other analytical fields we have standard materials, and these should not be hard to establish. Amongst those that we use is a homogeneous pyrophyllite from the Manuels deposit near St. John's.

Progress towards these objectives requires active collaboration between research organizations using VIRS data, and Government Geological Surveys, with their mandate to provide public information, are ideally poised to lead such an effort.

ACKNOWLEDGEMENTS

We thank Phoebe Hauff of Spectral International Inc., for her assistance in becoming Terraspec owners, and also for her insight into these methods, their potential and their complications.

REFERENCE

THOMPSON, A.J.B., HAUFF, P.L., & ROBITAILLE, A.J. 1996. Alteration mapping in exploration: application of shortwave infrared (SWIR) spectroscopy. *SEG Newsletter*, **39**, 15-27.

Analysis of gem treatments: comparison of nano-second and pico-second laser-induced breakdown spectroscopy

Nancy J. McMillan[1], Patrick Montoya, Carlos Montoya, & Lawrence Bothern
[1]Department of Geological Sciences, New Mexico State University, Box 30001, MSC 3AB, Las Cruces, New Mexico, 88003 USA (email: nmcmilla@nmsu.edu)

ABSTRACT: Gems are routinely treated with a variety of chemical additives to reduce defect visibility, enhance color, and improve stability. The ability to detect treatments is critical for the gem industry but is difficult because the analytical technique must be minimally destructive and sufficiently simple to be used by people throughout the gem industry as well as trained geochemical analysts. This work compares nano-second LIBS (Laser-Induced Breakdown Spectroscopy) to pico-second LIBS analysis of common gem treatments such as Be-diffused sapphires and rubies impregnated with leaded glass. Analytical conditions such as the wavelength of laser light and the environment of analysis (air, He, and Ar) are explored with the goal of determining the optimal analytical conditions. Data richness (amount of trace element information), data reproducibility, and damage to the gem are considered.

KEYWORDS: *gem, treatment, LIBS, sapphire, ruby, lead*

INTRODUCTION

Chemical treatments are commonly applied to imperfect gems to improve appearance and/or enhance the color. Although gem treatment is legal, dealers must disclose whether or not a specific specimen has been treated and what treatment has been applied. As treatment technology improves, the gem industry is increasingly aware of and sensitive to the presence of both disclosed and undisclosed treated gems in the marketplace. Thus, there is a need to be able to reliably detect chemically treated gems with a minimally-destructive technique.

LASER-INDUCED BREAKDOWN SPECTROSCOPY (LIBS)

In LIBS analysis, a pulsed laser is focused on the gem surface. The laser energy ablates a small amount of gem material which burns in a short-lived plasma. As the plasma cools, excited electrons decay into lower-energy orbitals, releasing energy in the form of photons in the ultraviolet-visible-infrared range. This light is collected by optic fiber, diffracted, and recorded as a spectrum, generally between 200 and 1000 nm.

This paper explores the trade-offs of gem damage during LIBS analysis and data quality under a variety of analytical conditions. Two lasers, a Big Sky Laser Technology (now Quantel USA) Nd-YAG nano-second laser operated at its fundamental wavelength of 1064 nm, and a Raydiance, Inc., pico-second laser operated at its fundamental wavelength of 1552 nm as well as harmonics at 776, 517.2, and 388 nm, are used in separate LIBS systems. Furthermore, the use of inert gas environment (He or Ar) is explored to increase peak intensities at lower laser power and sample damage.

RESULTS

The pico-second laser causes significantly less damage to the stone than the nano-second laser; however, fewer trace element peaks may be observed in the pico-second LIBS spectra (Fig. 1). The sensitivity of the pico-second LIBS system to trace elements may be enhanced in Ar or He, with a better lens system than currently employed, or by using the harmonic wavelengths. These parameters are under investigation.

The utility of LIBS analysis for two common gem treatments is illustrated

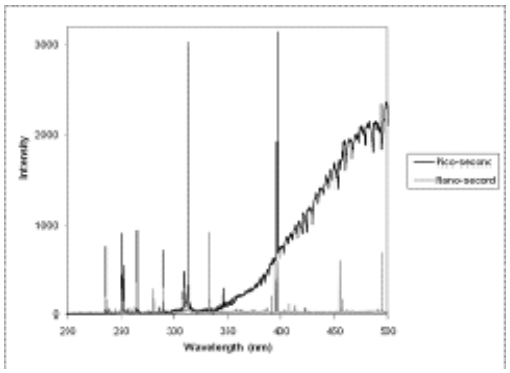

Fig. 1. Comparison of pico-second (black) and nano-second (gray) spectra from a faceted and polished aquamarine. Note that the nano-second spectrum has more peaks (from more elements) and far less continuum than the pico-second spectrum.

here using nano-second analyses in air. Rubies are sometimes impregnated with Pb-containing glass to render imperfections invisible (McClure *et al*. 2003). Because natural ruby has very low concentrations of Pb, detection of significant Pb indicates that glass at the gem surface has been analyzed. Fig. 2 presents LIBS spectra of six rubies, three of which have Pb peaks, indicating treatment with glass impregnation.

Since the 1990s, orange sapphires that have been diffused with Be have been found on the gem market (Emmett *et al*. 2003). Similar to leaded rubies, Be-diffused sapphires are easy to detect with LIBS because natural sapphires have low concentrations of Be (Emmett *et al*. 2003). Figure 3 shows LIBS spectra of six sapphires, three of which show the presence of Be at the dominant 313.1 nm peak. Further analyses are underway, in order to compare the pico-second LIBS spectra to their nano-second counterparts, to test different harmonic wavelengths of the pico-second laser, and to explore the use of Ar or He environment to reduce damage and increase peak intensity.

CONCLUSIONS

LIBS analysis of gem treatments has several advantages over traditional techniques, including:

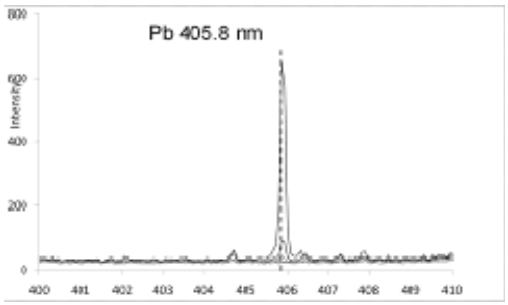

Fig. 2. Nano-second LIBS spectra of six rubies. The dominant Pb peak at 405.8 nm is marked.

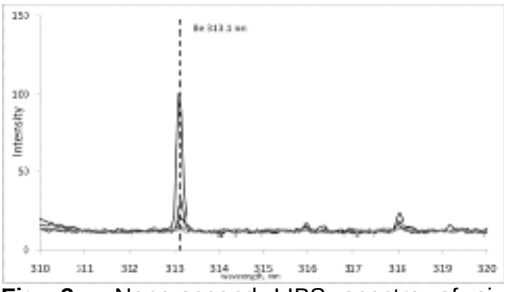

Fig. 3. Nano-second LIBS spectra of six sapphires. The dominant Be peak at 313.1 nm is marked.

(1) immediate and simple analysis;
(2) minimal damage;
(3) sensitivity to common gem chemical treatments.

If appropriate analytical protocols are developed, LIBS will have a place in the field of gem analysis to detect and monitor chemical treatments in the gem trade industry.

ACKNOWLEDGEMENTS

We gratefully acknowledge support from grants from the State of New Mexico Department of Economic Development and the collaboration of Raydiance Inc.

REFERENCES

EMMETT, J.L., SCARRATT K., MCCLURE S.F., MOSES T., DOUTHIT T.R., HUGHES R., NOVAK S., SHIGLEY J.E., WANG W., BORDELON O., & KANE R.E. 2003. Beryllium diffusion of ruby and sapphire. *Gems & Gemology*, **39**, 84-135.

MCCLURE, S.F., SMITH, C.P., WANG, W., & HALL, M., 2003. Identification and durability of lead-glass-filled rubies. *Gems & Gemology,* **42**, 22-34.

Laser ablation chemical analysis LIBS and LA-ICP-MS for geochemical and mining applications

R.E. Russo[1,2,3], J. Yoo[2], J. Plumer[1], J. Gonzalez[2], & X. Mao[3]
[1]*A3 Technologies, 1201 Technology Dr, Aberdeen, MD, 21001 USA*
[2]*Applied Spectra 46661 Fremont Blvd, Fremont, CA, 94538 USA*
[3]*Lawrence Berkeley Lab Berkeley, CA, 94720 USA (e-mail*: rerusso@appliedspectra.com)

ABSTRACT: Laser ablation has advanced to the stage of providing routine chemical characterization and analysis of solid samples without sample preparation. Advances in precision and accuracy allow a suite of applications from qualitative surveying to accurate quantization to age dating. Real-time in the field measurements without consumables make this approach a modern day 'green technology' for characterization and analysis. Two common implementations of laser ablation chemical analysis include LIBS (Laser Induced Breakdown Spectroscopy) which provides on the order of ppm detection, and LA-ICP-MS (Laser Ablation Inductively Coupled Plasma Mass Spectrometry), which provides ppb level sensitivity for most elements in the periodic table. Significant improvements in accuracy over XRF (x-ray fluorescence) are available for complex geological and mining samples. Commercial LIBS and ICPMS instruments are manufactured with integrated measurement protocols appropriate to a particular application. Data treatment chemometric processes are embedded in software making the laser ablation analysis technology more intuitive for the end-users.

KEYWORDS: *laser ablation, LIBS, ICP-MS, real-time analysis, instrumentation*

INTRODUCTION

This presentation will summarize developments in laser ablation with emphasis on LIBS (laser induced breakdown spectroscopy) and inductively coupled plasma mass spectrometry (ICP-MS) as analytical tools for real time chemical analysis (Fig. 1) (Russo *et al.* 2005). Laser ablation has become a prominent analytical technique over the past decade with applications crossing into many scientific disciplines, including geoscience, environmental, and forensics, among others (Baudelet, *et al.* 2007; Gonzalez *et al*. 2008). Laser ablation is a direct sampling technique by which a high energy laser is focused on the surface of a material and atoms, ions, and particles are ejected. The particles, which are chemically representative of the bulk sample, are then transported into an ICP-MS for analysis. In LIBS, a luminous, short-lived plasma is created on the sample surface by the focused laser beam and its emission spectra are analyzed to provide both qualitative and quantitative chemical compositional analysis (Cremers *et al.* 2006; Miziolek *et al.* 2006). Laser ablation based analysis is instantaneous, allowing real-time chemical composition analysis. Commercial systems are available for laboratory and field measurements.

LA offers several advantages over digestion/solution analyses such as 1) reduction in isobaric interferences, 2)

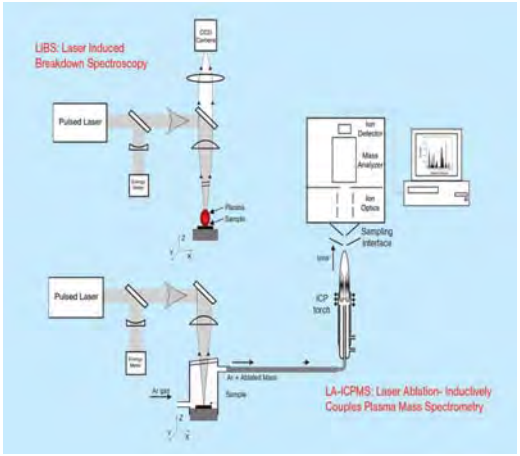

Fig. 1. Laser ablation with LIBS and LA-ICP-MS configurations.

reduction in sample size requirements, 3) a reduction in sampling time and 4) and the elimination of the need for acids further reducing potential for contamination and health risks. In addition, when compared to digestion and dissolution methods, researchers have reported similar precision and accuracy in the analysis of numerous samples; as a result, LA-ICP-MS is now the method of choice for elemental analysis, including geochemical analyses (Poitrasson *et al*. 2003).

This paper presents an overview of the current research issues and commercialization efforts related to laser ablation for chemical analysis, discusses several fundamental studies of laser ablation using time-resolved shadowgraph and spectroscopic imaging, and describes recent data using nanosecond laser pulsed ablation sampling for ICP-MS and LIBS. Efforts towards commercialization of field based LIBS systems also will be described.

LIBS ANALYSIS

Several applications will be described based on measurements obtained with two LIBS system that have been engineered and manufactured for industrial use. Our data illustrate how LIBS can answer a multitude of real-world needs for the rapid chemical analysis of various substances, including geological samples. The experiments were performed using RT100-HP and RT100-B commercial LIBS systems from Applied Spectra, Fremont, CA. These two instruments are similar, both acquire instantly a spectrum from a single laser shots, but they include different optical spectrographs. RT100-HP incorporates a high-performance Czerny Turner spectrograph attached to an image intensifier with timing control to select the gate width and delay for optimal analysis. This spectrograph has a dual grating turret, which allows the user to choose a spectral window with relevant spectral resolution (200 nm at resolution of 0.8 nm; or 40 nm at resolution of 0.1 nm). The other instrument RT100-B incorporates a broadband Echelle spectrograph with an intensified CCD camera that instantly acquires a wide span of spectrum from 200 to 900 nm at resolution ~0.05 nm. The RT 100-B allows discrimination of classes of compounds whereas the RT 100 HP is ideally suited for quantitative analysis of selected elements. Each model can be configured into a field-portable Pella-case design. We used the RT100-B to perform quantitative determination of lead in 12 different samples; several representative LIBS spectra from are shown in Figure. 2. For these measurements, we used 20 mJ laser pulses focused into 100 μm ablation spots.

Even though there seem to be a substantial degree of similarity between the spectra in Figure 2, they are all individually different. We applied a chemometric algorithm known as the principal component analysis (PCA) to compare and categorize these spectra. The results are presented in Figure 3 as a projection of our data from a multicomponent space onto coordinates of the two first principal components. It is evident that separation of high-lead samples from low-lead samples is easily achieved in this way. Therefore, a simple task of classifying samples into high or low lead groups can be fulfilled very rapidly and even without a need for standard calibration.

LIBS can be used for field screening on

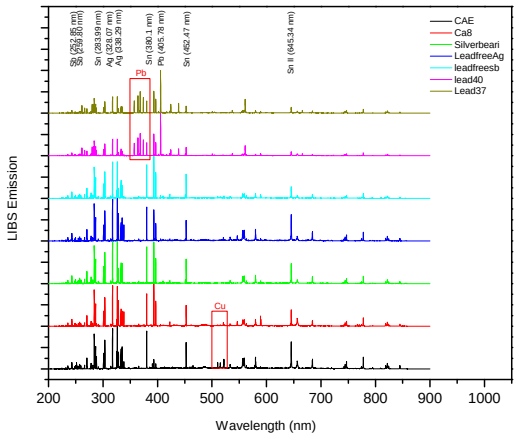

Fig. 2. Example broadband LIBS spectra.

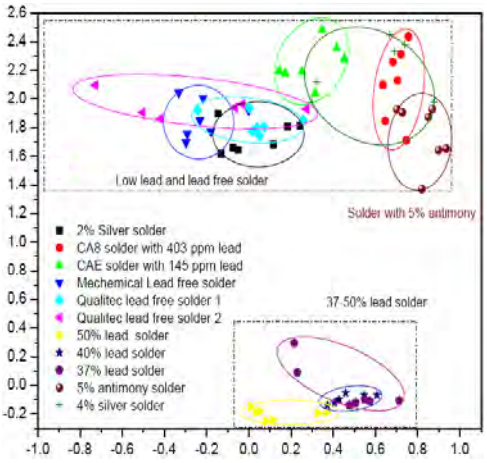

Fig. 3. PCA classification of samples.

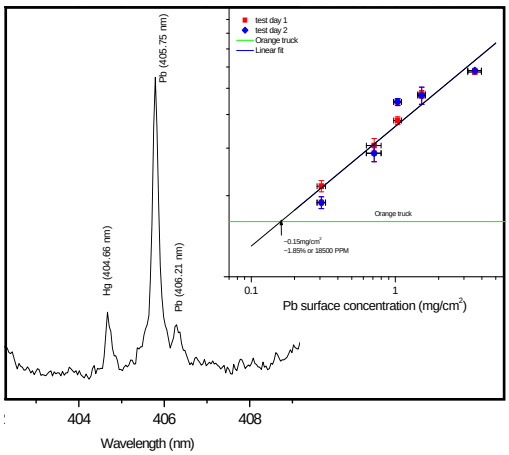

Fig. 4. Pb and Hg LIBS emission lines. Insert set.is analytical working curve analysis.

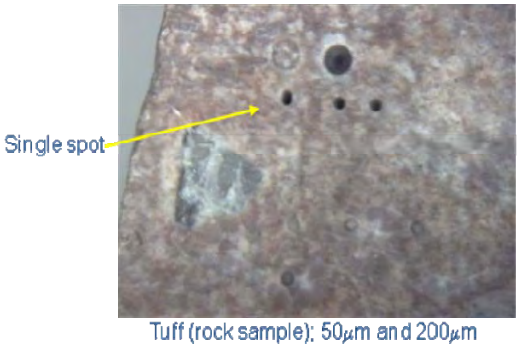

Fig. 5. Tuff sample with several laser sampled locations.

a qualitative level or for quantitative analysis. As example of quantitative analysis, we utilized the RT100-HP for measuring lead in the NIST 2579 reference sample

A portion of a spectrum that includes emission lines of mercury and lead is shown in Figure 4; the insert is a calibration plot for lead in this sample set. In general, LIBS provides detection on the ppm level for most elements; in this case on the order of 30 ppm for lead in glass based matrices. For higher sensitivity, LA-ICP-MS provide ppb detection.

Both LIBS and LA-ICP-MS offer spatial and depth resolution. A single laser shot provides an instantaneous measurement of approximately several nanograms to micrograms of sample. For spatial analysis, the laser is focused to several tens of microns and scanned across a surface. For depth analysis (including inclusions), the laser is pulsed repetitively at a single location to drill a channel into the sample (Fig. 5).

CONCLUSIONS

LA-ICP-MS and LIBS instruments can be used for fast and sensitive analysis of a wide variety of samples of interest to the geochemical and mining industries. Localized microanalysis with lateral and depth profiling is easily realized. Either traditional one-element calibration or multivariate chemometrics can be applied for qualitative or quantitative determination of elements in the samples. LIBS and LA-ICP-MS provide real-time chemical analysis with no sample preparation, across both laboratory and field applications. Companies including Applied Spectra and A3-Technologies have begun marketing LIBS systems for diverse applications. Integrated hardware and software allows user friendly applications within a completely integrated platform.

REFERENCES

BAUDELET M., BOUERI M., YU J., MAO S., PISCITELLI V., MAO X., & RUSSO R. 2007. Time-resolved ultraviolet laser-induced breakdown spectroscopy for organic material analysis. *Spectrochimica Acta* Part B: *Atomic Spectroscopy*, **20**,1329-1334.

CREMERS, D.A. & RADZIEMSKI, L.J. 2006. *Handbook of Laser Induced Breakdown Spectroscop. J.* Wiley & Sons, New York

GONZALEZ, J., OROPEZA, D., MAO, X.L., & RUSSO, R.E. 2008. Assessment of the precision and accuracy of thorium (^{232}Th) and uranium (^{238}U) measured by quadrupole based-inductively coupled plasma-mass spectrometry: comparison of liquid nebulization, nanosecond and femtosecond laser ablation. *Journal of Analytical Atomic Spectrometry*, **23**, 229-234.

MIZIOLEK, A.W., PALLESCHI, V., & SCHECHTER, I. (eds.) 2006. *Laser-Induced Breakdown Spectroscopy (LIBS), Fundamentals and Applications.* Cambridge University Press, UK.

POITRASSON, X.L., MAO, S.S., FREYDIER, R., & RUSSO, R.E. 2003. Comparison of ultraviolet femtosecond and nanosecond laser ablation inductively coupled plasma mass spectrometry analysis in glass, monazite, and zircon. *Analytical Chemistry*, **75**, 6184-6190.

RUSSO, R.E., GONZALEZ, J., & LIU, C.Y. 2005. Laser ablation: LIBS and ICP-MS. *Lab Plus International*.

In-situ Mössbauer spectroscopy on Earth, Mars, and beyond

Christian Schröder[1], Göstar Klingelhöfer[1], Richard V. Morris[2], Bodo Bernhardt[3], Mathias Blumers[1], Iris Fleischer[1], Daniel S. Rodionov[1,4], & Jordi Gironés López[1]

[1]Institut für Anorganische Chemie und Analytische Chemie, Johannes Gutenberg-Universität, Staudinger Weg 9, D-55099, Mainz GERMANY (e-mail: schroedc@uni-mainz.de)

[2]Astromaterials Research and Exploration Science, NASA Johnson Space Center, Mail Code KR, 2101 NASA Parkway, Houston, TX 77058, USA

[3]Von Hoerner & Sulger GmbH, Schlossplatz 8, D-68723 Schwetzingen GERMANY

[4]Space Research Center IKI, Moscow RUSSIA

ABSTRACT: Iron occurs naturally as Fe^{2+}, Fe^{3+}, and, to a lesser extent, as Fe^{0}. Many fundamental (bio)geochemical processes are based on redox cycling between these oxidation states. Mössbauer spectroscopy provides quantitative information about the distribution of Fe among its oxidation states, identification of Fe-bearing phases, and relative distribution of Fe among those phases. Determination of Fe^{3+}/Fe_{Total} and the identification of iron hydroxide mineral phases, for example, provide evidence for aqueous activity on the surface of Mars. Metallic iron identified in several rocks investigated on Mars suggests a meteoritic origin. These Mössbauer spectra were obtained with portable, miniaturized spectrometers on board the NASA Mars Exploration Rovers. Because of their backscattering measurement geometry, the instruments are directly placed on the sample surface to be analyzed by a robotic arm. In field studies on Earth, similar instruments have been used for the in situ study of green rust in soil, and as a prospecting tool and process monitor during field testing of precursor hardware for lunar in situ resource utilization (oxygen production). An advanced version of the Mars spectrometer has a new detector system permitting shorter measurement times and the capability for simultaneous acquisition of X-ray fluorescence spectra to determine elemental compositions.

KEYWORDS: *Mössbauer spectroscopy, MIMOS IIa, Mars Exploration Rover, In-situ resource utilization, X-ray fluorescence spectroscopy*

INTRODUCTION

Iron is one of the most abundant elements in the universe. Mössbauer (MB) spectroscopy is an established laboratory technique and a powerful tool to study Fe-bearing substances. The surface of Mars is Fe-rich compared to Earth, and a miniaturized MB spectrometer (MIMOS II) was developed for its robotic exploration as part of NASA's Mars Exploration Rover (MER) mission (Klingelhöfer *et al.* 2003). The capability of simultaneous acquisition of X-ray Fluorescence (XRF) spectra has been added. This new instrument, capable of both mineralogical and chemical applications (Klingelhöfer *et al.* 2008) is briefly described and then a few examples of extraterrestrial and terrestrial applications are presented.

MIMOS IIA INSTRUMENT DESCRIPTION

Mössbauer Spectroscopy

Available textbooks and reviews provide a detailed introduction to MB spectroscopy (e.g., Hawthorne 1988; Burns 1993). MB spectra provide quantitative information about the distribution of Fe among its oxidation and coordination states (e.g., octahedrally coordinated Fe^{3+}), identification of Fe-bearing phases, relative distribution of Fe among those phases, and can help to constrain crystallinity and particle size.

MIMOS IIa

MIMOS IIa is an advanced version of the MER instruments (Klingelhöfer *et al.* 2003) operating continuously since landing in January 2004. A new detector system has been implemented, inherited from the Alpha Particle X-ray Spectrometer (APXS), also part of the MER payload. This Si Drift Detector system provides higher energy resolution and increased

signal-to-noise ratio relative to the MER instruments, reducing measurement times and enabling the simultaneous acquisition of XRF spectra (Klingelhöfer *et al.* 2008). A ^{57}Co radioactive source provides the 14.4keV MB γ-rays and other energies for X-ray excitation. Acquisition of both 6keV and 14keV MB spectra enables depth selective measurements because of different attenuation coefficients (Fleischer *et al.* 2008). MIMOS IIa is set up in backscattering geometry to render sample preparation unnecessary; the instrument is simply placed on the surface to be analyzed, which is particularly useful for outdoor and in-situ applications. The instrument has a field of view of ~15 mm in diameter. Its main parts are a sensor head and an electronics board. A PC is necessary to start/stop measurements and for data read out. Wireless connection to the PC is possible. Power can be supplied via the mains in the lab, or a car battery, generator or solar cells in the field. The instrument, excluding PC and power supply, weighs less than 500 g.

MARS EXPLORATION

A "Follow-the-Water" strategy has been adopted for Mars Exploration. Hoehler *et al.* (2007) suggested a "Follow-the-Energy" approach. The primary objective of the MER mission is to explore two sites on Mars where water may once have been present, and to assess past environmental conditions at those sites and their suitability for life (Squyres *et al.* 2003).

Rock and Soil Classification

Rocks and soils (no implication of the presence or absence of organic materials or living matter intended) investigated with MERs *Spirit* and *Opportunity* in Gusev crater and at Meridiani Planum, respectively, were divided into classes on the basis of their chemical composition measured with the APXS and into subclasses on the basis of their Fe-bearing mineralogical composition and Fe^{3+}/Fe_{Total} ratios determined with the MB spectrometers (Ming *et al.* 2006, 2008; Morris *et al.* 2006a, 2006b, 2008). The distribution of igneous minerals (olivine and pyroxene) versus secondary minerals (hematite) and Fe^{3+}/Fe_{Total} ratios are a measure of weathering/alteration (e.g., Schröder *et al.* 2004).

Geologic Mapping

The APXS and MB in-situ dataset from individual stratigraphic units can be placed in a geologic context when reconciled with the MER remote sensing Miniature Thermal Emission Spectrometer (Mini-TES; McSween *et al.* 2008) and Panoramic Camera (e.g. Farrand *et al.* 2008) datasets. Adding orbital imagery enabled the first field reconnaissance geologic mapping on another planetary surface (Crumpler *et al.* 2009).

Habitability/Astrobiological Implications

Olivine in dust and soil suggests that physical rather than chemical weathering processes dominate on contemporary Mars (Morris *et al.* 2004), and the apparent global distribution of olivine-bearing dust and soil (Yen *et al.* 2005) reflects the overall extremely arid conditions on Mars. By contrast, aqueous minerals identified in outcrop rocks such as the Fe oxyhydroxide goethite in the Columbia Hills in Gusev crater (Morris *et al.* 2006a) or the Fe hydroxide sulfate jarosite at Meridiani Planum (Klingelhöfer *et al.* 2004) provide evidence for wet conditions in the past. Jarosite forms only at low pH and constrains environmental conditions. The abundance of ferrous versus ferric minerals provides further astrobiological implications because redox cycling of Fe, for example, can provide energy for microbial metabolism (e.g., Schröder *et al.* 2006).

Meteorites

Several meteorites were identified on Mars on the basis of their Fe metal and troilite contents (Schröder *et al.* 2008, 2009). Compared to the Moon, meteorites have a greater chance to survive impact on Mars because of its atmosphere. Compared to Earth, the current extremely arid climate on Mars lets meteorites

persist for much longer times and thus accumulate. Landis (2009) suggested that iron meteorites may be collected to provide steel as a construction resource on Mars for future human exploration.

LUNAR IN SITU RESOURCE UTILIZATION

Some essential consumables must be produced from lunar surface materials to enable a sustained, long-term presence of humans on the Moon. Oxygen, for example, can be produced by hydrogen reduction of metal cations (primarily Fe^{2+}) bonded to oxygen in the lunar regolith to metal (Fe^0) with the production of water. The hydrogen source is residual hydrogen in fuel tanks of lunar landers. Electrolysis of the water produces oxygen and hydrogen (which is recycled). Oxygen yield can be calculated by quantitative MB measurements of Fe distribution among oxidation states in the regolith before and after hydrogen reduction. Mounted on a rover, for example, MB spectrometers can also be used as prospecting tools to select the optimum feedstock for the oxygen production plants (e.g., high total Fe content and easily reduced phases). Both applications were demonstrated during the NASA Outpost Precursor for ISRU and Modular Architecture (OPTIMA) field test on Mauna Kea, Hawaii, in 2008.

TERRESTRIAL APPLICATIONS

Characterization of Particulate Matter

Airborne particles collected with filters distributed across Vitoria, Brazil were analyzed by MB spectroscopy, whereby certain Fe-bearing minerals indicated different pollution sources. For example, hematite comes mostly from iron ore pellet plants, pyrite from handling and storing coal in the industrial area, and magnetite is related to steelwork plants (de Souza *et al.* 2001).

Monitoring of Fougerite in the Field

Iron mixed-valence materials such as 'green rust' and fougerite are sensitive to air exposure and soil pollution by nitrates. A MIMOS instrument autonomously lowered or raised within a plexiglas tube, which was put down a bore hole, allowed to study their formation and distribution in situ as a function of depth in soil (e.g. Rodionov *et al.* 2006).

SUMMARY

A miniaturized MB spectrometer MIMOS II was developed for the robotic exploration of Mars, where it provided fundamental information about mineralogical composition and alteration processes, helped to classify rocks and soils, aided geologic mapping, was instrumental in assessing habitability of past and present environments, and identified potential construction resources for future human explorers. The applicability of the instrument as a process monitor for oxygen production and prospecting tool for lunar ISRU has been demonstrated. The characterization of air pollution sources and the study of mixed-valence materials as a function of depth in soil are examples of terrestrial in situ applications. MIMOS IIa with additional XRF capability will open up new applications.

ACKNOWLEDGEMENTS

The development and realization of MIMOS IIa was funded by the German Space Agency DLR under contracts 50QM99022, 50QX0603, and 50QX0802. The project has been supported by the Technische Universität Darmstadt and the Johannes Gutenberg-Universität Mainz.

REFERENCES

BURNS, R.G. 1993. Mössbauer Spectral Characterization of Iron in Planetary Surface Materials. In: PIETERS C.M. & ENGLERT P.A.J. (eds.), *Remote Geochemical Analysis: Elemental and Mineralogical Composition*, Cambridge University Press, UK, 539-556.

CRUMPLER, L. *et al.* 2009. Field Reconnaissance Geologic Mapping of the Columbia Hills, Gusev Crater from MER Spirit Rover and HiRISE Observations. *Lunar and Planetary Science*, **40**, 2045.

DE SOUZA JR., P.A. *et al.* 2001. On-line and in-situ characterization of iron phases in particulate matter. *Proceedings of the Air & Waste Management Association's 94th Annual Conference*, paper **569**, session AB-2d, 11p.

FARRAND, W.H. *et al.* 2008. Rock Spectral

Classes Observed by the Spirit rover's Pancam on the Gusev Crater Plains and in the Columbia Hills. *Journal of Geophysical Research*, **113**, E12S38, doi:10.1029/2008JE003237.

FLEISCHER, I. *et al.* 2008. Depth selective Mössbauer Spectroscopy: Analysis and simulation of 6.4 keV and 14.4 keV spectra obtained from rocks at Gusev crater, Mars, and layered laboratory samples. *Journal of Geophysical Research*, **113**, E06S21, doi:10.1029/2007JE003022.

HAWTHORNE, F.C. 1988. Mössbauer Spectroscpy. *Reviews in Mineralogy*, **18**, 255-340.

HOEHLER, T.M. *et al.* 2007. A "Follow the Energy" Approach for Astrobiology. *Astrobiology*, **7**, 819-823.

KLINGELHÖFER, G. *et al.* 2003. Athena MIMOS II Mössbauer spectrometer investigation. *Journal of Geophysical Research*, **108**(E12), 8067, doi:10.1029/2003JE002138.

KLINGELHÖFER, G. *et al.* 2004. Jarosite and Hematite at Meridiani Planum from Opportunity's Mössbauer Spectrometer. *Science*, **306**, 1740-1745.

KLINGELHÖFER, G. *et al.* 2008. The Advanced Miniaturised Mössbauer Spectrometer MIMOS IIa: Increased Sensitivity and New Capability for Elemental Analysis. *Lunar and Planetary Science*, **39**, 2379.

LANDIS, G.A. 2009. Meteoritic steel as a construction resource on Mars. *Acta Astronautica*, **64**, 183-187.

MCSWEEN, H.Y. *et al.* 2008. Mineralogy of volcanic rocks in Gusev crater, Mars: Reconciling Mössbauer, APXS, and Mini-TES spectra. *Journal of Geophysical Research*, **113**, E06S04, doi:10.1029/2007JE002970.

MING, D.W. *et al.* 2006. Geochemical and mineralogical indicators for aqueous processes in the Columbia Hills of Gusev crater, Mars. *Journal of Geophysical Research*, **111**, E02S12, doi:10.1029/2005JE002560.

MING, D.W. *et al.* 2008. Geochemical Properties of Rocks and Soils in Gusev crater, Mars: Results of the Alpha Particle X-ray Spectrometer from Cumberland Ridge to Home Plate. *Journal of Geophysical Research*, **113**, E12S39, doi:10.1029/2008JE003195.

MORRIS, R.V. *et al.* 2004. Mineralogy at Gusev Crater from the Mössbauer Spectrometer on the Spirit Rover. *Science*, **305**, 833-836.

MORRIS, R.V. *et al.* 2006a. Mössbauer mineralogy of rock, soil, and dust at Gusev crater, Mars: Spirit's journey through weakly altered olivine basalt on the plains and pervasively altered basalt in the Columbia Hills. *Journal of Geophysical Research*, **111**, E02S13, doi:10.1029/2005JE002584.

MORRIS, R.V. *et al.* 2006b. Mössbauer mineralogy of rock, soil, and dust at Meridiani Planum, Mars: Opportunity's journey across sulfate-rich outcrop, basaltic sand and dust, and hematite lag deposits. *Journal of Geophysical Research*, **111**, E12S15, doi:10.1029/2006JE002791.

MORRIS, R.V. *et al.* 2008. Iron mineralogy and aqueous alteration from Husband Hill through Home Plate at Gusev Crater, Mars: Results from the Mössbauer instrument on the Spirit Mars Exploration Rover. *Journal of Geophysical Research*, **113**, E12S42, doi:10.1029/2008JE003201.

RODIONOV, D. *et al.* 2006. Automated Mössbauer spectroscopy in the field and monitoring of fougerite. *Hyperfine Interactions*, **167**, 869-873.

SCHRÖDER, C. *et al.* 2004. Weathering of Fe-bearing minerals under Martian conditions, investigated by Mössbauer spectroscopy. *Planetary and Space Science*, **52**, 997-1010.

SCHRÖDER, C. *et al.* 2006. Fe Mössbauer spectroscopy as a tool in astrobiology. *Planetary and Space Science*, **54**, 1622-1634.

SCHRÖDER, C. *et al.* 2008. Meteorites on Mars observed with the Mars Exploration Rovers. *Journal of Geophysical Research*, **113**, E06S22, doi:10.1029/2007JE002990.

SCHRÖDER, C. *et al.* 2009. Santorini, Another Meteorite on Mars and Third of a Kind. *Lunar and Planetary Science*, **40**, 1665.

SQUYRES, S.W. *et al.* 2003. Athena Mars rover science investigation. *Journal of Geophysical Research*, **108**, 8062, doi:10.1029/2003JE002121.

YEN, A.S. *et al.* 2005. An integrated view of the chemistry and mineralogy of martian soils. *Nature*, **436**, 49-54.

Archaeometry in the House of the Vestals: analyzing construction mortar with portable infrared spectroscopy

Jennifer Wehby[1] & Samuel E. Swanson[1]

[1]University of Georgia, Department of Geology, Athens, GA, 30601 USA
(e-mail: Jennifer.Wehby@gmail.com)

ABSTRACT: The aim of this study was to test portable infrared spectroscopy for non-destructive analysis of ancient construction mortar. Mortar samples from the House of the Vestals, in Pompeii, Italy, were initially examined with traditional analytical techniques, including X-ray fluorescence, X-ray diffraction and thin section analysis. These techniques were used to establish mineralogical and chemical profiles of the samples and to verify the results of experimental field methods. Results showed the lime-based binder was composed of calcite, and the volcanic sand aggregate contained clinopyroxene, plagioclase, sanidine and olivine crystals.

Field analysis of the mortar *in situ* consisted of near-infrared (NIR) reflectance spectrometry with a portable FieldSpec®3 spectroradiometer. The instrument's detectors operate in the shorter wavelengths (300nm – 2500nm), which are useful for analysing and identifying carbonates; most of the silicates were not detected within the NIR range. Statistical analysis of NIR spectral data indicated the key variances between samples fell within ~2000 – 2200nm and ~2250 – 2375nm, approximately where the major absorption bands appeared in a reference sample of pure calcite. This suggests the binder component of mortar is potentially useful for distinguishing different mortar types, and that this method of non-destructive analysis of the mortar *in situ* shows some promise.

KEYWORDS: *near-infrared, portable, spectroscopy, mortar, Pompeii*

INTRODUCTION

Since 1995 the Anglo-American Project in Pompeii (AAPP) has been carrying out excavations and architectural analysis of one of ancient Pompeii's city blocks. This block, labelled insula VI.1, contains a mix of residential, commercial and industrial properties which survive as upstanding walls to a height of up to 3m. In its final phase, the House of the Vestals in Pompeii, Italy, had grown to its full extent by incorporating several smaller properties, evolving into one of the largest domestic structures in Pompeii (Jones and Robinson 2005). One of these smaller properties, VI.1.25 (Fig. 1) contains several different types of mortar, currently distinguished by color, which represent different construction phases. This structure presents a unique opportunity to test if and how the composition of calcium carbonate varies in each mortar type and how well these differences can be distinguished with portable infrared analysis. This mineral is well resolved with near-infrared spectroradiometers and should show subtle differences in the shape and intensity of absorption spectra because of subtle differences in composition and structure (Ellis 1930).

METHODS

From July 7-18, 2008, a near-infrared

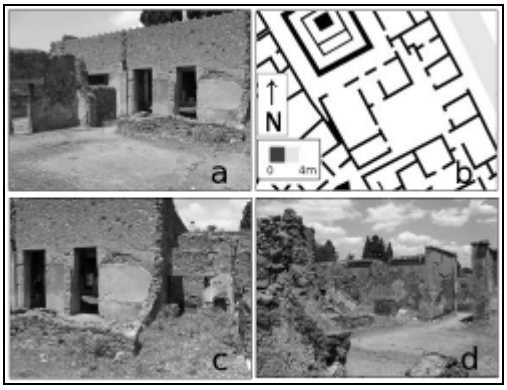

Fig. 1. House of the Vestals, structure VI.1.25, various views and plan map.

reflectance spectroscopy study of mortar was conducted *in situ* in the House of the Vestals using a portable spectroradiometer. These dates included three days of equipment set-up and testing and six days of analysis. Following the field tests in Pompeii, portable IR analysis was conducted on reference mortar samples collected during the 2007 field season of the AAPP. The hypothesis tested in this project is that individual construction phases will show differences in the absorption and reflectance features in near-infrared spectra of mortar, especially in the bands associated with $CaCO_3$.

Analysis was conducted with a FieldSpec®3 portable spectroradiometer, manufactured by Analytical Spectral Devices, Inc. This instrument measures, in a field setting, infrared energy reflected at short-wavelengths, including the visible and near-infrared (VNIR) and short-wave infrared regions (SWIR). The instrument contains three detectors: a VNIR detector, from 350 – 1050nm, and SWIR 1, from 1000 – 1800nm, and SWIR 2, 1800–2500nm (ASD 1999). The detectors are connected to the instrument with a single fiber optic cable that contains 19 fibers for each detector. The cable is inserted into a "pistol grip", a device that secures and directs the fiber optic cable during analysis. It can be either hand-held or mounted on a tripod; both configurations were tested (Figs. 2 and 3).

The instrument is controlled by an IBM Think Pad® laptop computer via a wireless network, utilizing ASD's proprietary software package. For this study, reference standard readings were collected before each sample reading to ensure consistent equipment function and to establish atmospheric conditions.

Fig. 2. Hand-held configuration of the FieldSpec®3. with the author taking a reference measurement.

Fig. 3. Tripod configuration of the FieldSpec 3® with the author taking a target sample reading.

Fluorescence analysis of dissolved organic matter (DOM) in landfill leachates

Caixiang Zhang[1], Yanxin Wang[1], & Zhaonian Zhang[2]
[1]MOE Biogeology and Environmental Geology Laboratory, China University of Geosciences, Wuhan, 430074 CHINA (e-mail:caixiangzhang@yahoo.com)
[2]Environmental monitoring of Yichang, Hubei, 443000 CHINA

ABSTRACT: Dissolved organic matter (DOM) in Landfill leachate contains a large number of unknown molecules. Due to its complex chemical compositions, the analysis of DOM in landfill leachates constitutes a major challenge and the questions of their geographic or climatic specificity as well as their evolution in time due to biodegradation processes will not be explained unless some effective characterization methods are designed. After undergoing fractionation by tangential ultrafiltration and resins XAD column, a fluorescence study of DOM originating from a domestic landfill (China) was present here. The distribution of dissolved organic carbon, UV absorbance, and humic-like fluorescence were different among all fractions and organic carbon absorbed on XAD-8 resin (HoN/B) contains more chromophores. Humic-like and fulvic-like fluorescence occurred in all fractions, but protein-like fluorescence only occurred in the colloidal fraction. Subtle differences in synchronous fluorescence spectra were observed among various fractions; this may indicate the occurrence of DOM degradation from higher to lower molecular weight. The results reported here have significance for further understanding the sources and nature of DOM in aquatic environments.

KEYWORDS: *Colloids, Dissolved organic matter, Fractionation, Fluorescence, Landfill leachate*

INTRODUCTION

Landfill leachate is an important point pollution source to water body, which contains DOM with a large number of unknown molecules that actively involve in biogeochemical and environmental processes (Chin *et al.* 1997). DOM not only plays an important role in freshwater systems for the mobility of toxic heavy metals and other pollutants but also may itself be a groundwater contaminant (Christensen *et al.* 1998).

Municipal landfill leachate typically contains dissolved organic carbon (DOC) concentrations up to several thousand (typically >1700 ppm), even in a landfill that is decades old (Christensen *et al.* 1998). More than 200 organic compounds have been identified in municipal landfill leachate (Paxe´us 2000). Therefore, an effective chemical characterization of landfill leachate by numerous analytical techniques requires a previous isolation procedure in order to remove possible interferences. In our previous study, we tested the advantage of the ultrafiltration and resins XAD column chromatography to fractionate leachates (Zhang 2007). In this paper, the UV and fluorescence spectroscopies are used to define the spectral prosperities of each group of compounds present in the landfill leachates.

MATERIALS AND METHODS

Leachates were collected from a landfill site (Wuhan, China), receiving compacted domestic wastes. Samples were pre-filtered by a microfilter device (1μm, Millipore) and sequently fractionated by tangential ultrafiltration into DOM (<0.45um labelled as R1-3) and <1kDa (labelled as R1-5) fractions. The DOM was separated into relative hydrophilic (HI) and hydrophobic (HO) fractions by XAD columns due to resin's different properties and to hydrophobic/hydrophilic interactions occurring between the resin and organic matter (Zhang 2007), including hydrophilic acids (HiA), hydrophobic acids (HoA), Hydrophobic neutrals and bases (HbN/B), hydrophilic

neutrals and bases (HiN/B) and polar components (pc) (shown in Fig. 1). All fractions were adjusted to pH 6-7 and analyzed for DOC (Elementar Liquitoc, Germany), UV_{254}(HP-1800) and fluorescence spectra (PerkinElmer LS55).

The EEM fluorescence spectroscopy involved scanning and recording of 23 individual emission spectra (220–510 nm) at sequential increments of 10 nm of excitation wavelength between 260 and 490 nm. The spectra were recorded at a scan speed of 1000 nm/min using excitation and emission slit bandwidths of 10 nm. Analyses were performed at a constant laboratory temperature of 22±3 ^{o}C, and blank water scans were run between every 10-20 analyses using a sealed distilled water cell.

The synchronous spectra (SF) were collected in the 260-460 nm excitation wavelength range using bandwidth of Δλ=20 nm between the excitation and emission monochromators. All SF and emission spectra were recorded with a 10 nm slit width on both monochromators. The scan speeds of spectra were 500 nm/min.

RESULTS AND DISCUSSION

Chemical analysis

Table 1 presents the results of fractionations of the DOM. The result of mass balance calculation of the DOC system shows that more than 55 % of the total DOC was retained by XAD-8 resin column, involving the portions of HoA and HbN/B, and DOC concentrations of the portion eluted by blackwashing (HoA) accounted for 47.4 % of total DOC, as compared with 26.25 % hydrophilic acids (HiA) of the total DOC. More than 11% of the total DOC passed through two resin columns, indicating that small molecular weight polar components were not absorbed onto by XAD-8 and XAD-4. The fractionation did cause potential loss of organic matter by permanent adsorption onto resin's polymers, which were 8.34 % for the XAD-8 resin and 6.41 % for the XAD-4 resin, respectively.

Characteristic peaks position

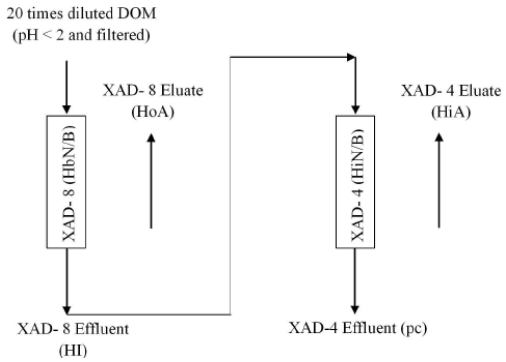

Fig. 1. Scheme of the tandem XAD-8/XAD-4 isolation procedure of DOM portion from the landfill leachate

Table 1

The chemical properties of the permeate after acidification and the filtered DOM and its fractions[a] isolated by XAD-8 and XAD-4

Parameters	Permeate	HO	HoA	HbN/B[c]	HI	HiA	HiN/B[c]	pc
DOC (mg/l)	355.90	198.39	168.71	29.68	157.51	93.41	22.81	41.29
%[b]		55.74	47.4	8.34	44.26	26.25	6.41	11.60
UV_{254} (cm^{-1})	0.913	-	0.302	0.162	0.198	0.046	0.286	0.009

[a] mass balance of DOC formulas: HO=HoA+HbN/B; HI=HiA+HiN/B+pc; DOM=HO+HI

[b] percentage over total DOC

[c] estimated by difference in mass balance

A typical fluorescence EEM results for leachate samples from R-landfill demonstrate five distinctive and intense fluorescence peaks in Figure 2, such as at Ex/Em=230–250/400–440 nm (labeled as "A"), which was relative to UV humic fraction identified in location to the diagnostic fluorescence centre observed previously; at Ex/Em=220–230/340–370 nm (labeled as "D"), a poorly understood fluorescent centre widely attributed to a component of the UV fulvic-like (Coble 1996); at Ex/Em=320–350/400–440 nm (labeled as "C"), which can be attributed to aromatic and aliphatic groups in the DOM fraction and commonly labeled as fulvic-like (Coble 1996); at Ex/Em=350–400/420–460 nm (labeled as "E"), which is attributed to humic-like and a final fluorescence centre at Ex/Em= 275–280/350–360 nm (labeled as "B"), which is attributed to the protein tryptophan, and widely observed in polluted river waters (Baker 2001; 2002) and clean estuaries (Mayer *et al.* 1999).

Synchronous fluorescence spectra of all fractions were similar shown in Figure 3, but showed differences in relative intensity of four characteristic peaks at about 285,

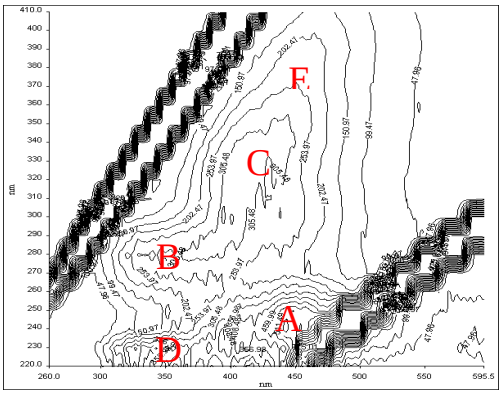

Fig. 2. EEM fluorescence contour and surface profile of the DOM isolated form landfill leachate.

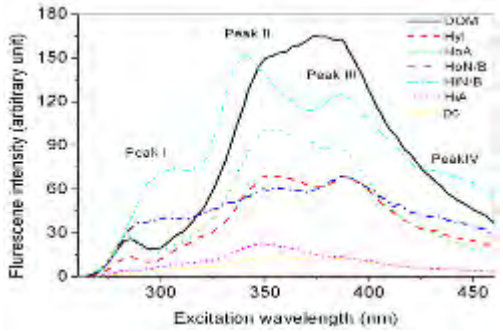

Fig. 3. SF spectra for original DOM and its six fractions at offsets of 20nm.

350, 385 and 434 nm. This is most likely caused by different concentrations of fluorophores in the DOM. In addition to possible DOM source differences, the λ_{max} for Peak I (B in Fig. 2 described above) can also depend on the $\delta\lambda$ used for the synchronous fluorescence (De Souza Sierra & Donard 1994). In our study, the λ_{max} was most commonly observed at about 285 mn, and this wavelength was used throughout the study to characterize Peak I. Peaks II and III are characteristic for fulvic acids and solution humic acids ("C" and "E" in Fig. 2 described above), whereas peak IV is associated with the presence of humic acids (F not shown in Fig. 2).

Synchronous fluorescence has the potential to provide useful information regarding the relative abundance of protein-like vs. fulvic-like DOM (Peak I / Peak II) and humic-like vs. fulvic-like DOM (Peak III/Peak II). Figure 4 shows the

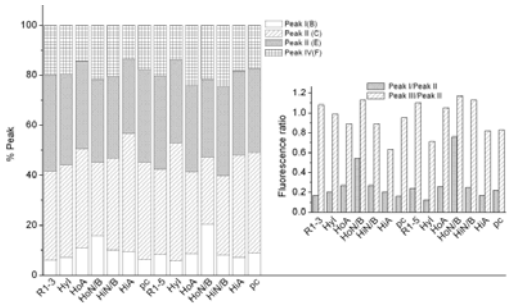

Fig. 4. The relative abundance (%) comparison between isolated fraction of R1-3 (05) and of R1-5 by XAD in the synchronous fluorescence spectra and the fluorescence index, Peak I/Peak II, Peak III/Peak II. Peak I-IV: 285, 350, 385, and 430 nm

relative abundance of each fraction isolated from leachate DOM. Fulvic-like acids and solution humic acids are dominant in each fraction isolated from DOM. The XAD resin could separate DOM into different fractions and higher ratio of Peak I/Peak II appeared in HoN/B and HiN/B, suggesting that N-containing chromophores can be adsorbed by XAD resins such as aliphatic amine, protein, amino-acid, pyrimidine.

In synchronous fluorescence spectra (Fig. 3) there are some shifts at 350 and 385 nm to shorter wavelengths as compared with original DOM. This shift in the maxima of fluorescence intensity from longer to shorter wavelengths is associated with a decreasing number of highly substituted aromatic nuclei (Miano & Senesi 1992). The calculated ratios of fluorescence intensity should be a measure of the degree of polycondensation and humification of DOM. Therefore, to the ratio were used as humification index here. Only two clearly distinguishable bands (Peak II and III) are needed to calculate the humification index because all samples were dominated by them (Figs. 3, 4). The greater ratio may be attributed to greater content of higher molecular weight organic matter in samples. The HoN/B fraction with highest humification indices was found in Figure 4. It was reasonable since humification indices of organic compounds adsorbing onto XAD-8 resin (humic substances)

should be higher than those of non-humic substances.

CONCLUSIONS

Emission-Excitation Matrix (EEM) fluorescence spectroscopy as a non-destructive and sensitive analytical technique was successfully applied in this study to characterize DOM in landfill leachte. The DOM is composed of complex mixture of organic compounds with different fluorescence properties. In particular, the EEM profiles of DOM show two well-defined peaks at Ex/Em=320-350 /400-420 nm, Ex/Em=320-350 /420–450 nm reasonably due to the presence of two different groups of fluorophores. An additional and less intense band at Ex/Em=280-290 /320-350 nm can be assigned to aromatic amino acids and phenol-like compounds.

The EEM profiles of fractions obtained by the isolation procedure of the DOM by the XAD resins showed that a fractionation was effective and the XAD-8 eluate is highly representative of the original DOM. Emission scan spectra of DOM and its fractions are featureless, whereas synchronous scan spectra show that the isolation procedure is efficient in separating the original DOM into fractions with different fluorescence properties. The synchronous scan spectra obtained with a wavelength offset of 20 nm present multicomponent samples such as the DOM fractions from landfill leachate.

The EEM fluorescence allows identifying major differences in fluorescent properties between fractions. However, the EEM fluorescence spectroscopy may become very time-consuming. For quick preliminary analysis, it is recommended that synchronous fluorescence spectra be used for distinguishing samples of DOM with different chemical properties.

ACKNOWLEDGEMENTS

The research work was financially supported by the National Natural Science Foundation of China (Grant for Outstanding Young Scholars No.40425001), and Wuhan Science and Technology Bureau (200860423203).

REFERENCES

BAKER, A. 2001. Fluorescence excitation–emission matrix characterization of some sewage- impacted rivers. *Environmental Science & Technology,* **35**, 948-953.

BAKER, A. & CURRY, M. 2004. Fluorescence of leachate from three contrasting landfills. *Water Research*, **38**, 2605-2613.

CHIN, Y.P., AIKEN, G.R., & DANIELSEN, K.M. 1997. Binding of pyrene to aquatic and commercial humic substances: The role of molecular weight and aromaticity. *Environmental Science & Technology*, **31**, 1630-1635.

CHRISTENSEN, J.B., JENSEN, D.L., GRON, C., FILIP, Z. *ET AL.* 1998. Characterization of the dissolved organic carbon in landfill leachate-polluted groundwanter. *Water Research*, **32**, 125-135.

COBLE, P.G. 1996. Characterization of marine and terrestrial DOM in seawater using excitation–emission matrix spectroscopy. *Marine Chemistry*, **51**, 325-346.

DE SOUZA SIERRA, M.M., DONARD, O.F.X., LAMOTTE, M., BELIN, C. *ET AL*. 1994. Fluorescence spectroscopy of coastal and marine waters. *Marine Chemistry*, **47**, 127-44.

MAYER, L.M., SCHICK, L.L., LODER, T.C. 1999. Dissolved protein fluorescence in two main estuaries. *Marine Chemistry*, **64**, 171-179.

MIANO, T.M., & SENESI N., 1992. Synchronous excitation fluorescence spectroscopy applied to soil humic substances chemistry. *Sci Total Environ*, 117/118, 41-51.

PAXE´US, N., 2000. Organic compounds in municipal landfill leachates. *Water Science and Technology*, **42**,323- 33.

ZHANG, C.X. 2007. PhD thesis. China University of Geosciences.

Innovation for the CHIM method

Liu Zhanyuan, Sun Binbin, Wei Hualing, Zeng Daoming, & Zhou Guohua
Institute of Geophysical and Geochemical Exploration, Langfang, Hebei, 065000, P.R. CHINA
(e-mail: Liu zhanyuan@igge.cn)

ABSTRACT: The method of the electro-geochemistry extraction (CHIM) for exploration has been continuously improved since it was used in China. The CHIM method is innovated through designing the new cathode receiver with solid absorbents, powered by battery in a low-voltage "dipole" mode with time controller. The innovated method has the following advantages: (1) Power for element receiver is independently supplied by a low-voltage "dipole" battery at each sampling site. The survey scale is not limited by electrical wires. The method can be applied in regional exploration. (2) The equipment is light-weight. (3) The cathode receiver with solid absorbents is easily operated in the field. (4) Time controller adopted is for standard time control at each sampling site.

KEYWORDS: CHIM, *dipole mode, time-control function The cathode receiver with the 'solid' absorbents, small scale*

INTRODUCTION

The method of the electro-geochemistry extraction (CHIM) was developed by Yus Ryss.

The CHIM method have been applied in exploration for hidden base metals, gold deposits since CHIM was introduced to China in the beginning of 1980s. The CHIM method became less used since the middle 1990s due to its heavy equipment, complicated operation, expensive cost and low efficiency etc. However the research on understanding of its mechanism and on improvements for its technology is continuously carried out. It was found that CHIM technology extracts signals of mineralization elements from materials surrounding the receiver. The signals are transported from ore deposits at depth to surface by other mechanisms in a long period of past processes, not driven by present electricity force. The renovation of the CHIM technique was based on this new knowledge. The anomalous elements can be extracted by a low voltage dipole focusing on a small diameter area.

THE NEW CATHODE RECEIVER

The new cathode receiver consists of the graphite pole and solid absorbents fixed in a plastic container (Figs. 1 and 2).

The shape of the new cathode receiver is a flat cylinder with a diameter of 12.8cm and a height of 2.8cm. The solid absorbents can put inside and take out by opening the cover (Fig. 2).

POWER SUPPLY BY LOW VOLTAGE DIPOLE

The cathode receiver and the anode were composed into a dipole system, powered by a low voltage battery (Fig.3). The distance of the anode-cathode is about 30~40cm. The receiver (cathode) is buried in the soils at a depth of 30~40cm. The anode stainless steel is installed directly over the receiver at the ground surface.

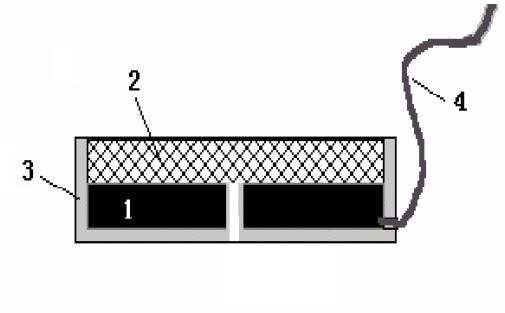

Fig. 1. Sketch map of the cathode receiver; 1-graphite-pole; 2-solid absorbent materials; 3-plastic container;4-electrical wire.

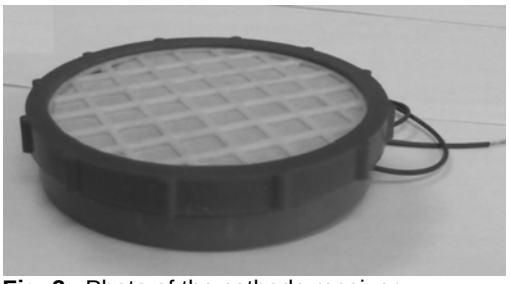

Fig. 2. Photo of the cathode receiver.

.

Fig. 3. Sketch of the 'Dipole CHIM' system.

TIME CONTROLER

We designed a time-controller for insuring the same extraction time at each sample station (Fig. 4). The power supply time is automatically controlled between zero to 24 hours.

A CASE STUDY

Figure 5 shows the results at Jinwozi gold deposit in Xinjiang (Wang *et al*. 2007). Samples were taken along a 15km long profile across the deposits. Sampling intervals are 500 m in 2001 and 100 m in 2002 respectively. The results indicate that anomalies of Au obtained by different intervals are obviously coexisting over the ore bodies. The previous CHIM powered by electrical generator can not used for such long profile survey.

CONCLUSIONS

(1) The innovation CHIM technology is based on extracting elements at a limited

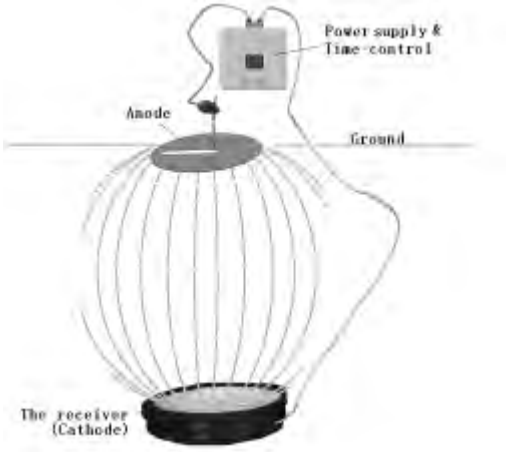

Fig.4. "Dipole CHIM" with time controller

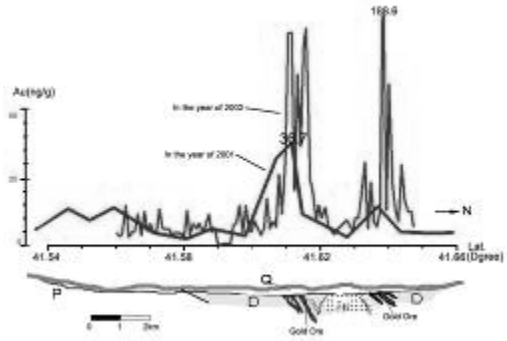

Fig. 5. Gold anomalies obtained by the innovation CHIM technique across the Jinwozi gold deposit in Xinjiang.

area surrounding the cathode, which the elements are transported from ore deposits at depth to surface by other mechanisms in a long past period of processes.

(2) The improved CHIM technology is enable to carry out survey not only at large scale but also at small scale.

(3) The improved CHIM technology with the time-controller can be used for standardization of sampling time.

(4) The improved CHIM technology has light equipment, convenient operation, low cost and high working efficiency, etc.

ACKNOWLEDGEMENTS

We would like to give our thanks to Dr. Wang Xueqiu for translating Chinese into English. Thanks are given to the Ministry

of Science and Technology for financial support (project No. 2007AA06Z133).

REFERENCES

Hamilton, S.M. 1998. Electrochemical mass transport in overburen: a new model to account for the formation of selective leach geochemical anoamalies in Glacial Terren. *Journal of Geochemical Exploration,* **63**, 155-172.

LEIZ, R.W. 1994. Ideal CHIM with the newly-Developed NEOCHIM electrode, V.S. *Exploration Geochemists*, **83**, P10-15.

MING, K. & XIAN-RONGCES, L. 2003. Improvement and applied results of geoelectrical chemistry methods. *Geology and Prospecting*, **5** (in Chinese).

MING, K., KUANG, C., & XIAN-RONGCES, l. 2006. Application of "DIPOLE CHIM" electrified by low voltage. *Geology and Prospecting*, **4** (in Chinese).

RYSS, Y. 1983. The methods of the electro-geochemistry extraction, *The Geologe Publish of China,* in Chinese, 1986, translating Russian into Chinese by ZHANG ZHAOYUAN & CUI LINPEI.

WANG, X., LIU Z., & YE, R. *et al.* 2003. Deep-penetrating geochemistry: A comparative study in the Jinwozi Gold Ore District, Xinjiang. *Geophysical & Geochemical Exploration*, **4** (in Chinese).

WANG, X., WEN, X., YE, R., LIU Z., SUN, B., ZHAO, S., SHI, S., & WEI, H. 2007. Vertical variation and dispersion of elements in arid desert regolith: a case study from the Jinwozi gold deposit, northwestern China. *Geochemistry: Exploration, Environment, Analysis*, **7**, 163-171.

ZHANYUAN, L., JIMIN, L., & AIMIN, C. 1997. Adiscussion on the action conditions of CHIM process. *Geophysical & Geochemical Exploration* , **2** (in Chinese).

ZHANYUAN, L., ZHIZHONG, C, & BINBIN, S. 2005. The processed of the carrier material in the cathode receiver. *Geophysical & Geochemical Exploration* , **5** (in Chinese) .

Sponsors

Symposium bags sponsor

ACME Analytical Laboratories Ltd.

Platinum sponsors

SGS

Anglo American

Gold sponsors

AREVA

Newmont – The Gold Company

Barrick

TGI3 Canada

Canada

Silver Standard

maxwell DATASHED

Actlabs

FREEWEST – Freewest Resources Canada Inc.

Silver sponsors

ODM – Exploring Heavy Minerals

Thermo Scientific

Innov-X Systems – Innovative XRF Technologies

APEGNB / APEGNB

OZ

xstrata zinc

Adex

Bronze sponsors

PotashCorp – Helping Nature Provide

International Association of Geochemistry – IAGC – Est. 1962

New Nouveau Brunswick – Natural Resources and Energy

Department of Geology, University of New Brunswick

IAG